ISSN 0736-5306

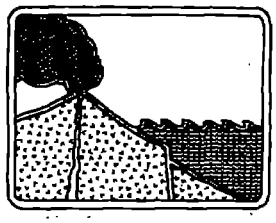

SCIENCE OF TSUNAMI HAZARDS

The International Journal of The Tsunami Society

Volume 15 Number 2 1997

NUMERICAL MODELING OF TRANS-PACIFIC TSUNAMIS: THE 1995 CHILE, THE 1996 ALEUTIAN, AND THE 1996 IRIAN JAYA TSUNAMIS 67

Yuichiro Tanioka and Masami Okada
Japan Meterological Research Institute, Tsukuba, Japan

THE 1994 SKAGWAY TSUNAMI TIDE GAGE RECORD 81

Dennis Nottingham, P.E.
Peratrovich, Nottingham and Drage, Inc., Anchorage, AK USA

LANDSLIDE-GENERATED TSUNAMI IN SKAGWAY, ALASKA 89

Zygmunt Kowalik
University of Alaska, Fairbanks, AK USA

THE JANUARY 1, 1996 SULAWESI ISLAND TSUNAMI 107

Efim Pelinovsky
Institute of Applied Physics, Nizhny Novgorod, Russia

Dede Yuliadi
Navy Hydro-Oceanographic Service, Jakarta, Indonesia

Gegar Prasetya and Rahman Hidayat
Tsunami Research Center, Jakarta, Indonesia

SCIENCE OF

TSUNAMI HAZARDS

PUBLICATION FORMAT INFORMATION

Typing area is 25 by 19 cm.

One-column text.

All text to be single-space.

Indent 5 spaces to start a new paragraph.

Page numbers in lower right hand corner in blue pencil.

**Top half of first page to contain title in CAPTIALS,
followed by authors and author affiliation centered on page.**

**Bottom half of first page to contain abstract with
heading ABSTRACT centered on page.**

Send original camera ready paper and a copy to

Dr. Charles Mader, Editor
Science of Tsunami Hazards
Mader Consulting Co.
1049 Kamehame Drive
Honolulu, Hawaii 96825-2860, USA

APPLICATION FOR MEMBERSHIP

THE TSUNAMI SOCIETY
P. O. Box 25218
Honolulu, Hawaii 96825, USA

I desire admission into the Tsunami Society as: (Check appropriate box.)

☐ Student ☐ Member ☐ Institutional Member

Name _____ Signature _____

Address _____ Phone No. _____

_____

Zip Code _____ Country _____

Employed by _____

Address _____

Title of your position _____

FEE: Student $5.00 Member $25.00 Institution $100.00

Fee includes a subscription to the society journal: SCIENCE OF TSUNAMI HAZARDS.

Send dues for one year with application. Membership shall date from 1 January of the year in which the applicant joins. Membership of an applicant applying on or after October 1 will begin with 1 January of the succeeding calendar year and his first dues payment will be applied to that year.

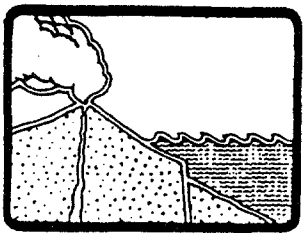

NUMERICAL MODELING OF TRANS-PACIFIC TSUNAMIS:

THE 1995 CHILE, THE 1996 ALEUTIAN, AND THE 1996 IRIAN JAYA TSUNAMIS

Yuichiro Tanioka and Masami Okada
Seismology and Volcanology Department,
Meteorological Research Institute, Tsukuba, 305 Japan

ABSTRACT

Numerical simulation of trans-Pacific tsunamis is tested for three large earthquakes (the 1996 Aleutian, 1995 Chile, and 1996 Irian Jaya earthquakes) which occurred in the last two years. Overall, the observed and computed maximum tsunami heights at tide gauges show relatively good agreement.

1. INTRODUCTION

In 1960, the tsunami from the Chilean earthquake propagated across the Pacific ocean and killed about 140 people in Japan. Since then, trans-Pacific tsunami have been studied extensively. In recent years, numerical modeling of trans-Pacific tsunami has been significantly developed (*Goto et al,* 1988, *Imamura et al.,* 1990, etc.). The numerical modeling has been tested for the 1964 Alaska and the 1960 Chile earthquakes but have never been tested for recent trans-Pacific tsunamis caused by large earthquakes. Recently, the fault parameters for large earthquakes are reliably estimated using various data, such as seismic, geodetic, or near-field tsunami data (*Tanioka, et. al,* 1995, *Tanioka, et al,* 1996). Since the fault parameters are accurately determined, we can now evaluate the numerical method of far-field tsunami critically by comparing observed and computed tsunami.

In last two years, tsunamis from three large earthquakes (the 1995 Chile, 1996 Irian Jaya, and 1996 Aleutian earthquakes) propagated across the Pacific ocean and were recorded at tide gauges in Japan. In this paper, we use those three earthquakes as test cases to test the numerical method for the trans-Pacific tsunami. The fault parameters of the earthquakes are carefully estimated from the available data.

2. METHOD

(1) Generation of Tsunami

The initial condition of a tsunami is the water surface displacement caused by ocean bottom deformation due to faulting. The fault motion of the earthquake can be described by the fault parameters: the location of the fault, geometry (strike, dip, and rake), the fault size (length and width), and the slip amount. From these fault parameters, the ocean bottom deformation can be computed using *Okada's* (1985) equations.

(2) Computation of Tsunami Propagation

A tsunami which is generated by a large earthquake can be treated as a linear long wave because the wavelength is substantially larger than the water depth. For tsunamis propagating a long distance such as across the Pacific ocean, the effects of Earth's sphericity and rotation (Coriolis force) must be also included. The integrated equations for linear long waves with the Coriolis force in the spherical coordinate system (longitude φ and colatitude θ) are

$$\frac{\partial Q_\varphi}{\partial t} = -\frac{gd}{R\sin\theta}\frac{\partial h}{\partial \varphi} - fQ_\theta$$
$$\frac{\partial Q_\theta}{\partial t} = -\frac{gd}{R}\frac{\partial h}{\partial \theta} - fQ_\theta \qquad (1)$$
$$f = 2\Omega\cos\theta$$

and

$$\frac{\partial h}{\partial t} = -\frac{1}{R\sin\theta}\left[\frac{\partial}{\partial\theta}(Q_\theta \sin\theta) + \frac{\partial Q_\varphi}{\partial \varphi}\right] \qquad (2)$$

where R is the radius of the earth, g is the acceleration of gravity, d is water depth, Ω is the rotation vector of the earth, h is the height of the water displaced from equilibrium position, and Q is the flow rate. We solved the above equations using finite-difference calculations on a staggered grid system. The grid size for the entire Pacific Basin must be carefully chosen to make the effects of numerical and physical dispersion equal. *Imamura et al*, (1990) showed that the choice of the grid size can be evaluated using the Imamura number, *Im*, defined as

$$\mathrm{Im} = \Delta x\sqrt{1-\left(C_0\,\Delta t/\Delta x\right)^2}\,\Big/2h \qquad (3)$$

where Δx is the grid size, Δt is the time step, and $C_0 = \sqrt{gh}$. The value of *Im* must be about 1 to simulate the linear Boussinesq equation using the finite difference computation for a linear long wave. We chose the grid size (Δx) of 5 minutes and the time step (Δt) of 5 seconds to satisfy the stability condition. Using Equation (3) for the above case, *Im* is 1.15 in the N-S direction, by assuming that the average depth is 4000m. In the E-W direction, *Im* varies with latitude and *Im* is 0.73-1.15 within the latitude between 50 and 0 degree. These results show that *Im* for the above case is about 1, so the 5 minute grid system on the Pacific Basin should make the numerical dispersion equal to the physical dispersion.

Near coastal areas, the bathymetry changes rapidly and can not be adequately represented by a 5 minute grid (- 10 km). Therefore, in the coastal areas (near the west coast of North America, the Aleutians, Hawaii, and Japan), 1 minute grid (- 2 km) spacing is used. In addition to that, 20 seconds grid (- 600 m) spacing is used near some of the tide gauge stations in Japan.

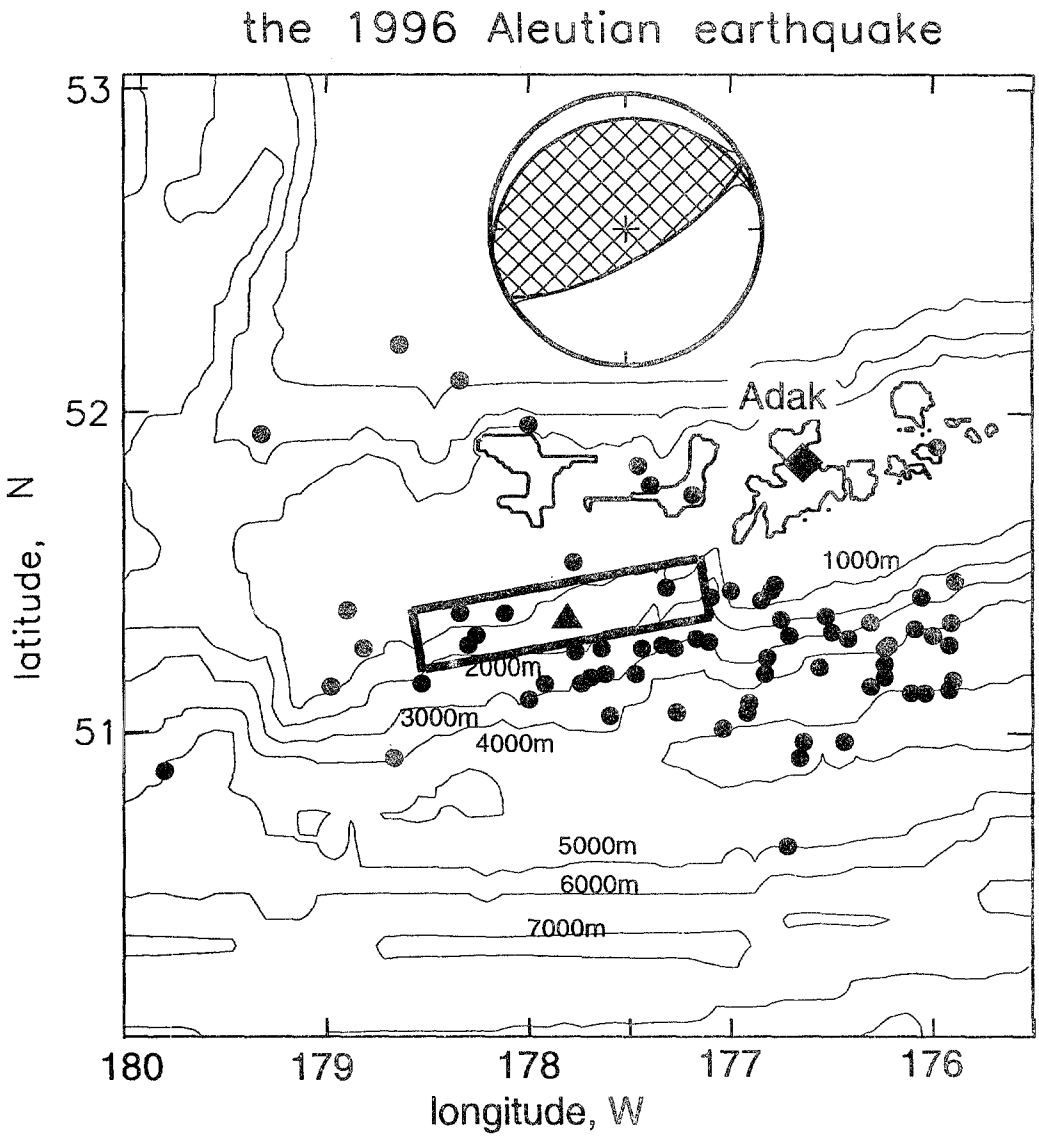

Figure 1. The focal mechanism and the preferred fault model of the 1996 Aleutian earthquake. The rectangle shows the location and size of the fault. A triangle is the epicenter of the mainshock. Circles are the epicenter of aftershocks. The diamond shows the tide gauge (Adak).

3. THE 1996 ALEUTIAN EARTHQUAKE

The Aleutian earthquake of June 10, 1996 (Ms 7.6, Mw 7.9) occurred off the Delarof Islands, Alaska (Figure 1). The NEIS Preliminary Determination of Epicenters (PDE) provides the source parameters: origin time, 04:03:35.48 GMT; epicenter, 51.564°N, 177.588°W; magnitude, Ms 7.6. The focal mechanism of the earthquake from the Harvard CMT catalog indicates thrust type faulting with a shallow dip angle (20°) (Figure 1). It generated a trans-

Pacific tsunami which was recorded at tide gauge stations in the west coast of North America, Hawaii and Japan. The source time function of the earthquake was determined by the Michigan group (*Tanioka and Ruff,* 1997) using teleseismic body waves. It shows the duration of 54 seconds, seismic moment of 7.3 X 10^{20} Nm and depth of 18 km. There is one near-field tsunami waveform recorded at a tide gauge station, Adak, about 100 km away from the epicenter (Figure 1). Using a pure thrust type fault (strike=260°, dip=20°, rake=90°) which is consistent with the focal mechanism, we computed the tsunami waveform at Adak for various fault sizes. The fault model which best explained the observed waveform is shown in Figure 1 (length 110 km, width 20 km, average slip 4 m). The epicenter is located near the center of the fault. The fault area is much smaller than the aftershock area (Figure 1).

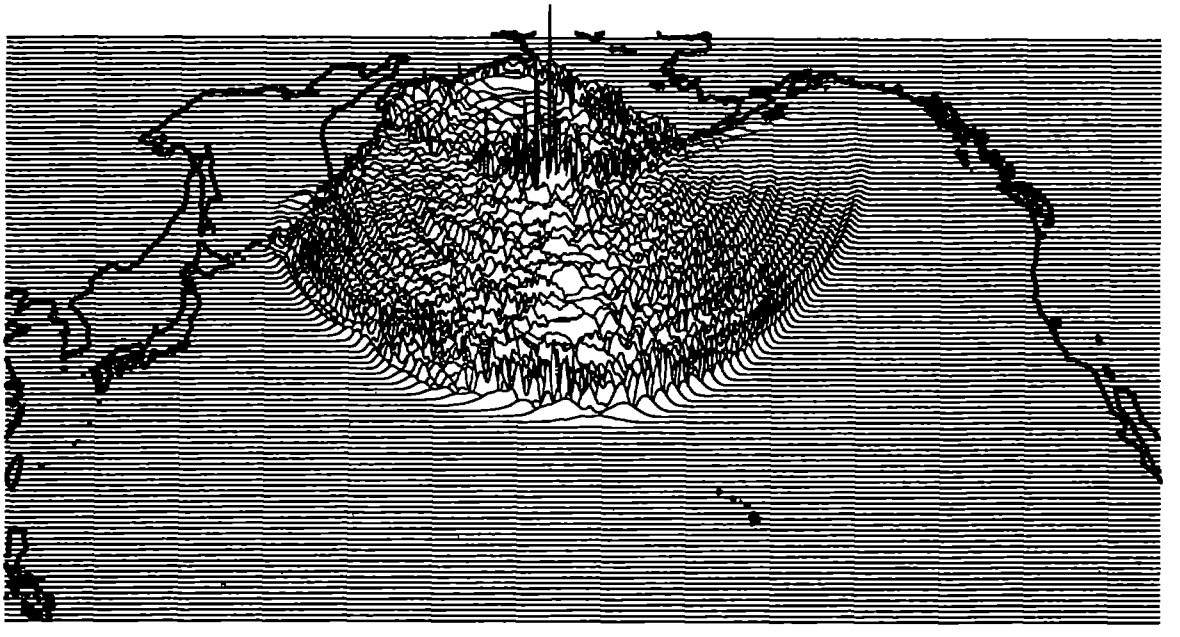

Figure 2. Snapshot of tsunami 3 hours after the 1996 Aleutian earthquake.

Using this fault model, we computed the trans-Pacific tsunami. Figure 2 shows a snapshot of tsunami propagation across the Pacific Ocean 3 hours after the earthquake. As can be seen in Figure 2, large tsunamis propagate toward Hawaii, but very small tsunamis propagate toward the west coast of North America. This is due to the directivity effect; tsunami heights are usually smaller in the direction parallel to the orientation (strike) of the fault (*Ben-Menahem and Rosenman,* 1972). Figure 3 shows a comparison of the observed and computed maximum tsunami heights at the tide gauges in Japan (Uragami, Owase, Omaezaki, and Chichijma), Hawaii (Honolulu, Kahului, and Hilo), and the west coast of North America (Arena Cove and Port Orford). The maximum tsunami height is the largest tsunami height

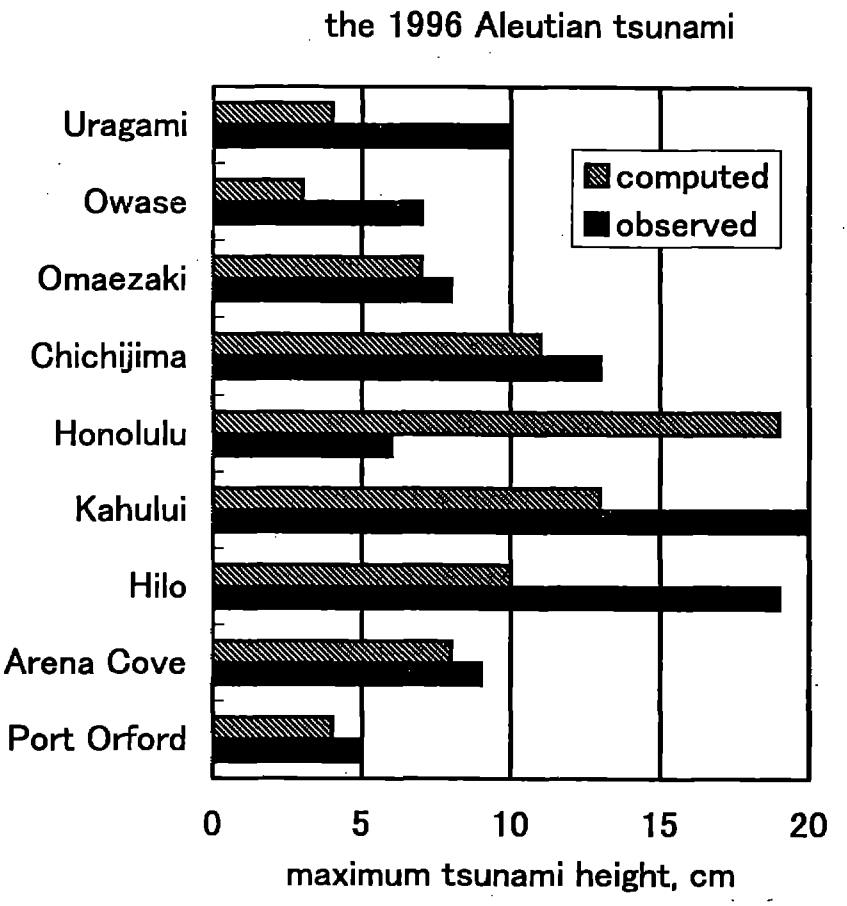

Figure 3. Comparison of observed and computed maximum tsunami heights at tide gauges in Japan, Hawaii, and the west coast of North America.

during the first 3 hours after the first peak. The observed and computed maximum tsunami heights fit well except at the Hawaiian stations. In Figure 4, we compare the observed and computed waveforms at three tide gauges. At Arena Cove and Chichijima, the observed and computed waveforms show very good agreement, but not at Hilo. This may suggest that a finer grid system or more accurate bathymetry near Hawaii is necessary to improve the accuracy of the model.

4. THE 1995 CHILE EARTHQUAKE

The Chile earthquake of July 30, 1995 (Mw 8.0) occurred off Antofagasta, Northern Chile (Figure 5). The NEIS Preliminary Determination of Epicenters (PDE) provides the source parameters: origin time, 05:11:23.6 GMT; epiceuter, 23.340°S, 70.294°W; magnitude, Ms 7.3. The focal mechanism of the earthquake (*Ruegg et al.,* 1996) indicates thrust type faulting with a shallow dip angle (19°) (Figure 1). *Ruegg et al*, (1996) also determined three subevents from

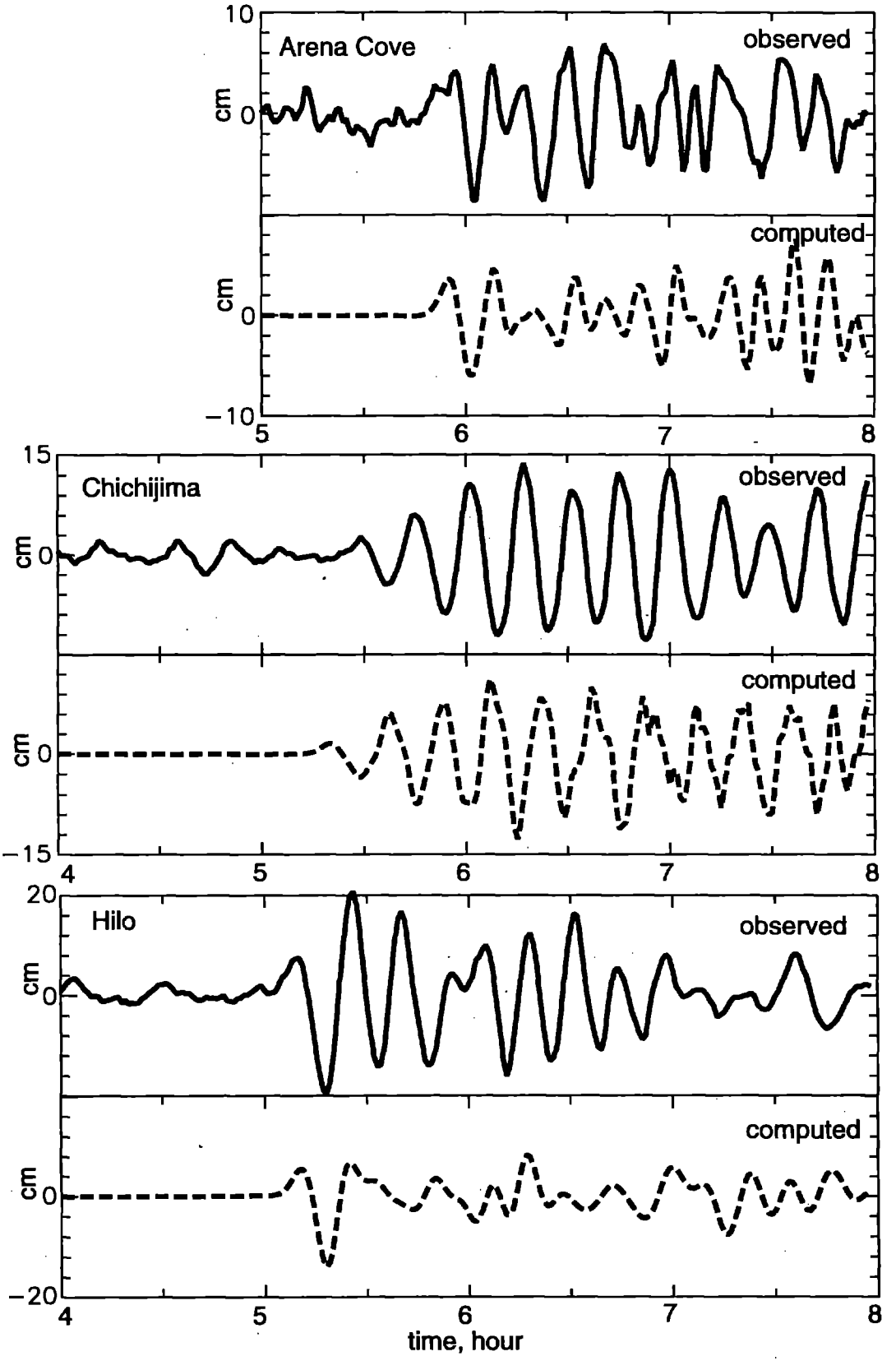

Figure 4. Comparison of observed and computed tsunami waveforms at three tide gauges.

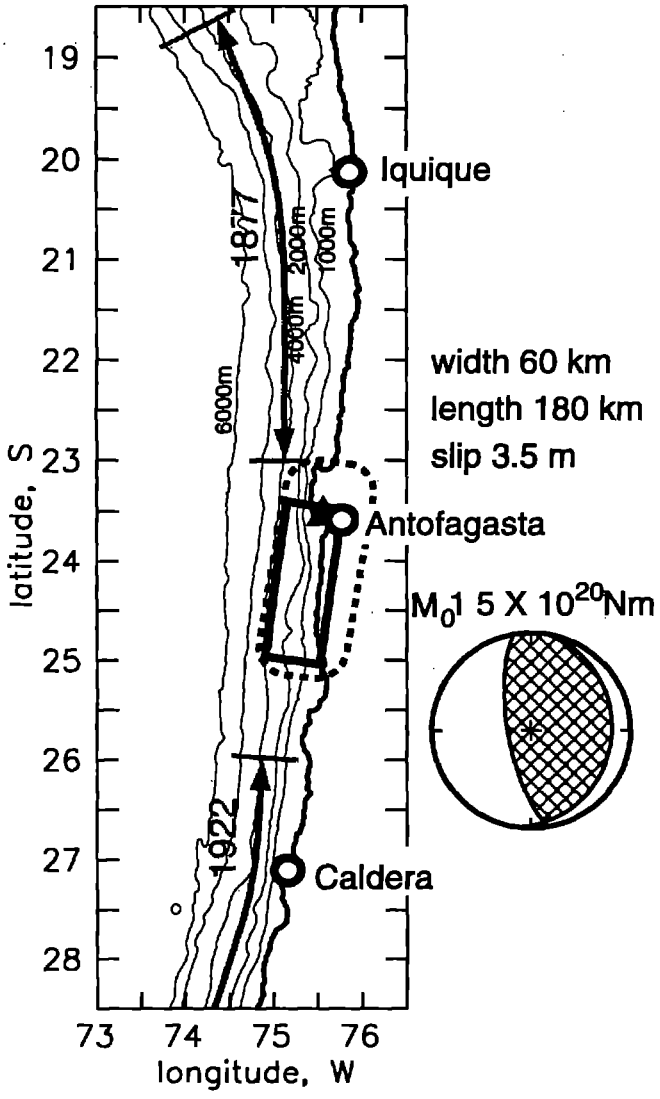

Figure 5. The preferred fault model and the focal mechanism of the 1995 Chile earthquake. The rectangle shows the location and size of the fault. A star is the epicenter of the mainshock. The dashed ellipse shows the aftershock area. Circles are tide gauges.

body wave analysis and suggested that the rupture propagated southward with a total rupture length of about 180 km. The total seismic moment is estimated as 9 X 10^{20} Nm. They also determined a fault width of 60 km and average slip of about 5m using the coseismic surface displacement field observed by the GPS network near the source region.

The 1995 Chile earthquake also generated large tsunamis. In addition to the coseismic displacement data (*Ruegg et al*, 1996), we used the tsunami waveforms recorded at three tide gauges in northern Chile (Figure 5) to determine the fault parameters. Using a thrust type fault (strike=8°, dip=20°, rake=107°), we computed the tsunami waveforms and the surface

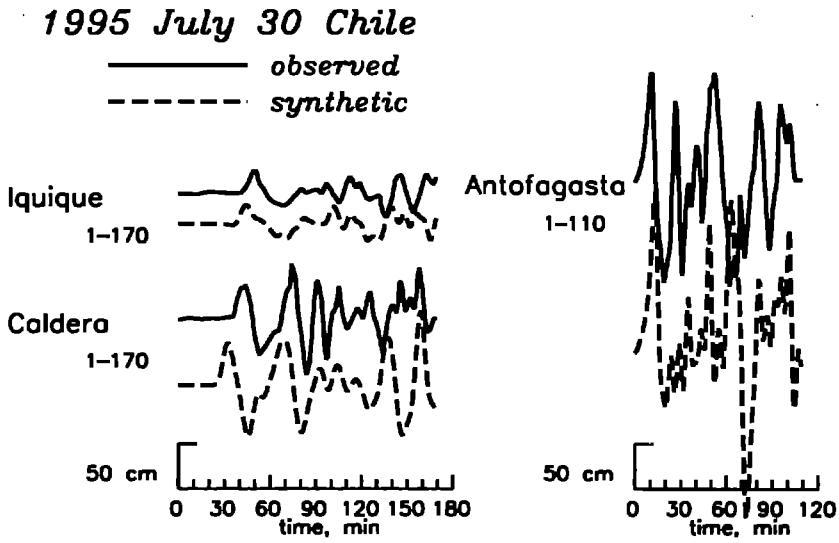

Figure 6. Comparison of the observed and computed tsunami waveforms

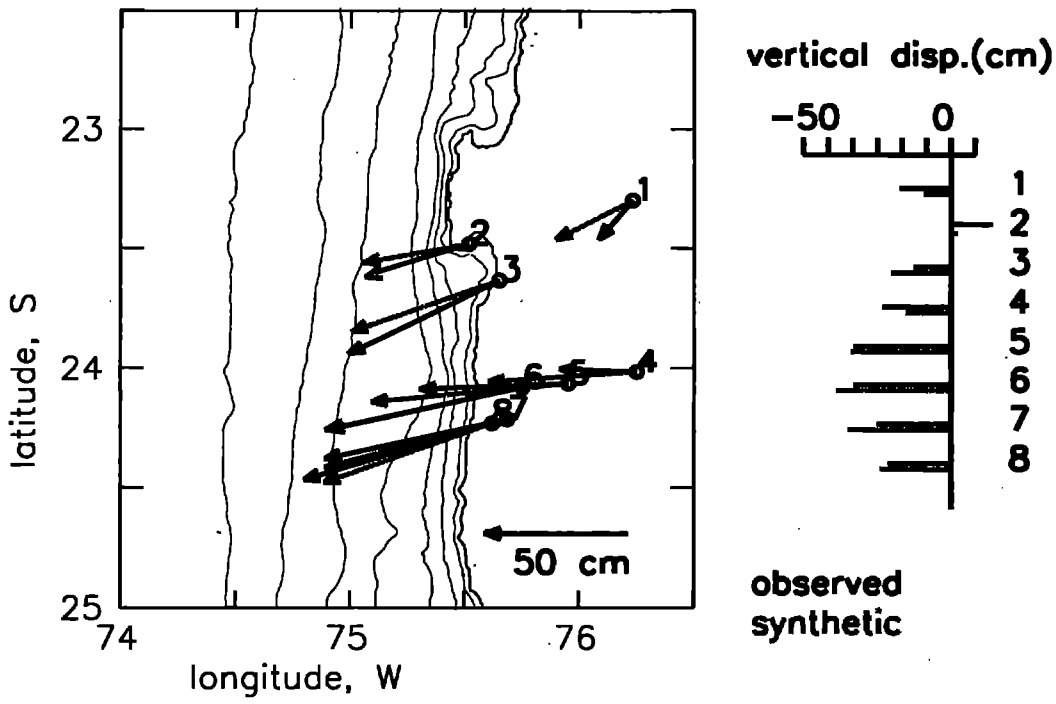

Figure 7. Comparison of the observed (*Ruegg et al.*, 1996) and computed coseismic displacement field. (left) Comparison of the horizontal displacements. (right) Comparison of the vertical displacements.

displacement field for various fault sizes and depths. The best fault model (length 180 km, width 60 km, slip 3.5 m) is shown in Figure 5. Figure 6 shows the computed tsunami waveforms also fit well with the observed waveforms. Figure 7 shows that the computed surface displacement field is consistent with the observed field. The seismic moment is 15 X 10^{20} Nm by assuming that the rigidity 4 X 10^{10} N/m^2. This result is consistent with the estimate from the body wave analysis. Tsunamis from the 1995 Chile earthquake propagated across the Pacific ocean and were recorded at tide gauge stations in Japan. We computed the traus-Pacific tsunami using the above fault model determined from seismic, coseismic displacement, and near-field tsunami data. Figure 8 shows that the observed and computed maximum tsunami heights during the 3 hours after the first arrival of the tsunami at tide gauges in Japan. Computed maximum tsunami heights are slightly greater than the observed maximum tsunami heights. More detail investigation is necessary to determine the cause of these small differences.

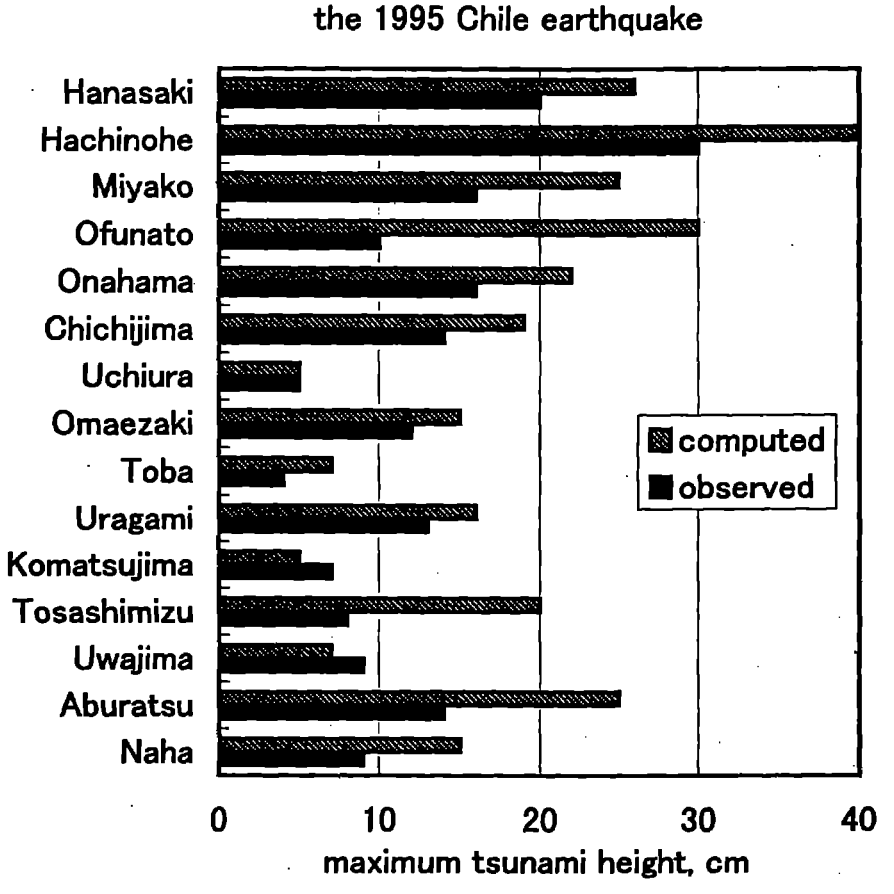

Figure 8. Comparison of the observed and computed maximum tsunami heights at tide gauges in Japan.

5. THE 1996 IRIAN JAYA EARTHQUAKE

The Irian Jaya earthquake of February 17, 1996 (Mw 8.1) occurred off Biak Islands, Indonesia (Figure 10). The NEIS Preliminary Determination of Epicenters (PDE) provides the source parameters: origin time, 05:59:30.55 GMT; epicenter, 0.891°S, 136.952°E; magnitude, Ms 8.1. The Harvard CMT focal mechanism of the earthquake indicates thrust type faulting with a very shallow dip angle (11°) (Figure 9). The source time function of the earthquake was determined by the Michigan group (*Tanioka and Ruff,* 1997) using teleseismic body waves. It shows a total duration of 50 seconds with an initiation phase of 18 seconds. The seismic moment is 18 X 10^{20} Nm. For this earthquake, we do not have a near-field tsunami waveform recorded at a tide gauge. *Stevens et al.,* (1996) observed the coseismic subsidence of Biak Islalld. Using this subsidence of Biak Island and the aftershock distribution, we estimated the fault size (length 200 km, width 75 km) (Figure 9). Assuming a seismic moment of 18 X 10^{20} Nm and a rigidity of 4 X 10^{10} N/m^2, the average slip is 3 m.

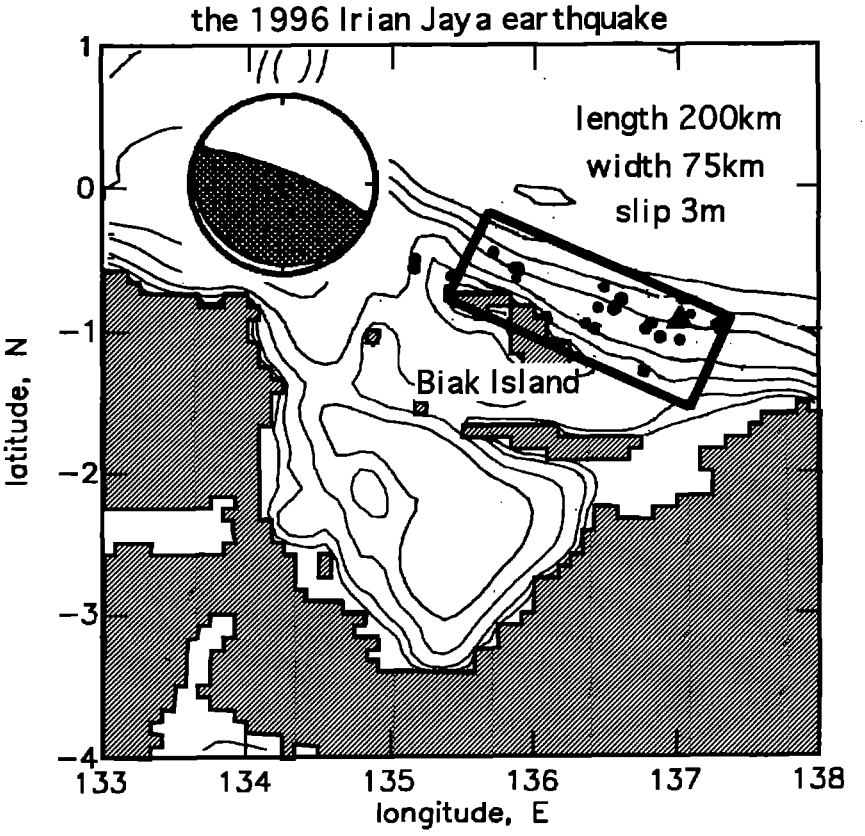

Figure 9. The focal mechanism and the preferred fault model for the 1996 Irian Jaya earthquake. The rectangle shows the location and size of the fault. A triangle represents the epicenter of the mainshock. Circles shows the epicenters of the aftershocks.

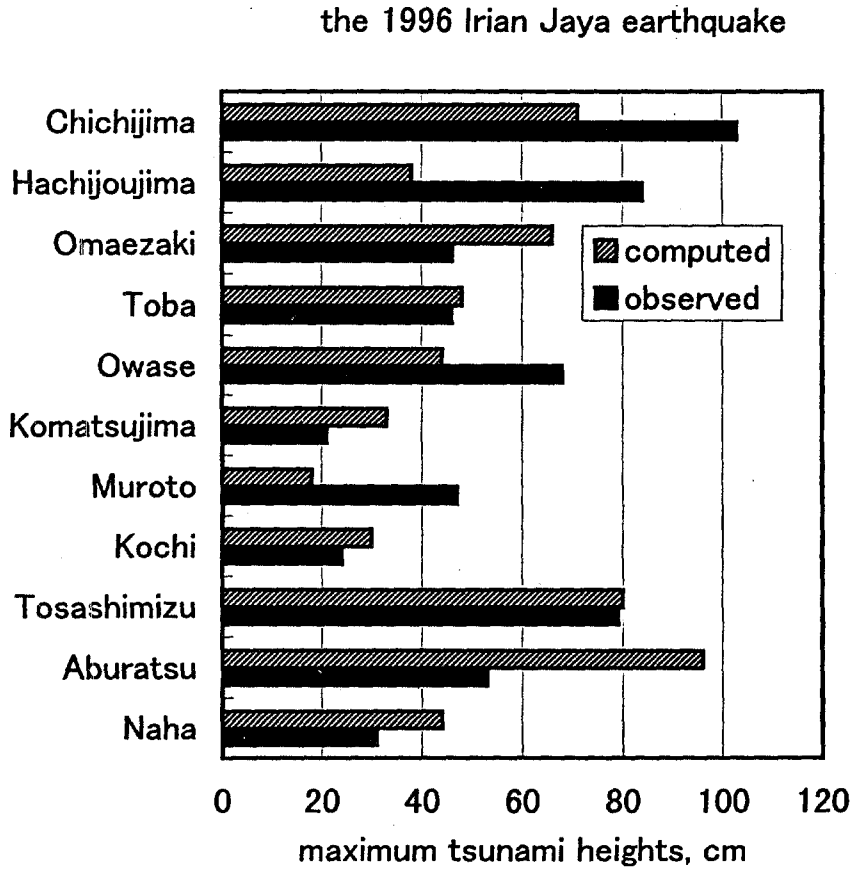

Figure 10. Comparison of the observed and computed maximum tsunami heights at tide gauges in Japan.

Tsunamis from the 1996 Irian Jaya earthquake were also recorded at tide gauge stations in Japan. We computed the tsunami using a pure thrust type fault (strike=115°, dip=10°, rake=90°) with the above fault dimensions. Figure 10 shows that the observed computed maximum tsunami heights at tide gauge stations in Japan. Overall, the observed and computed maximum tsunami heights are in good agreement.

6. CONCLUSION

Overall, the numerical simulation of trans-Pacifie tsunamis performed well. The difference between the observed and computed maximum tsunami heights was less than a factor 2 except for a few tide gauge stations in each event. Using more accurate bathymetry near those stations may improve the accuracy of the computation. This type of numerical simulation of trans-Pacific tsunami will be a useful tool for a tsunami warning system in the near future.

Acknowledgments.

We thank Dr. F.I. Gonzalez at PMEL, NOAA for providing the tide gauge records in U SA. We also thank Dr. S.E. Barrientos for providing the tide gauge records in Chile. The tide gauge records in Japan for the 1996 Aleutian earthquake was provided by Mr. H. Tatehata. The discussion with Dr. J.M. Johnson was helpful.

REFERENCE

Ben-Menahem, A. and M. Rosenman, Amplitude pattern of tsunami waves from submarine earthquakes, *J. Geophy. Res , 77,* 3097-3128, 1972.

Imamura, F., N. Shuto, and T. Goto, Study of numerical simulation of the transoceanic propagation; Part 2: characteristics of tsunami propagating over the Pacific Ocean, *Jishin 2, 43,* 389-402, 1990.

Goto, T., F. Imamura, and N. Shuto, Study of numerical simulation of the transoceanic propagation of tsunami Part 1: governing equation and mesh length, *Jishih 2, 41,* 515-526, 1988.

Okada, Y., Surface deformation due to shear and tensaile faults in a half space, *Bull. Seism. Soc. Am., 75,* 1135-1154, 1985.

Ruegg, J. C. et al., The Mw=8.1 Antofagasta (North Chile) earthquake of July 30, 1995: First results from teleseismic and gcodetic data, *Geophys. Res. Lett., 9,* 917-920, 1996.

Stevens, C et al., Coseismic deformation of the Feb 1996 Biak earthquake sequence determined from GPS measurements, *EOS. Trans. AGU, 77,* S184, 1996.

Tanioka, Y., and L.J. Ruff, Source time function, *Seismo. Res. Lett.*, (in press).

Tanioka, Y., K. Satake, and L.J. Ruff, Total analysis of the 1993 Hokkaido Nansei-oki earthquake using seismic wave, tsunami, and geodetic data, *Geophys. Res. Lett., 22,* 9-12, 1995.

Tanioka, Y. , L. J. Ruff, and K. Satake, The Sanriku-oki, Japan, earthquake of December 28, 1994 (Mw 7.7): Rupture of a different asperity from a previous earthquake, *Geophys. Res. Lett., 12,* 1465-1468, 1996.

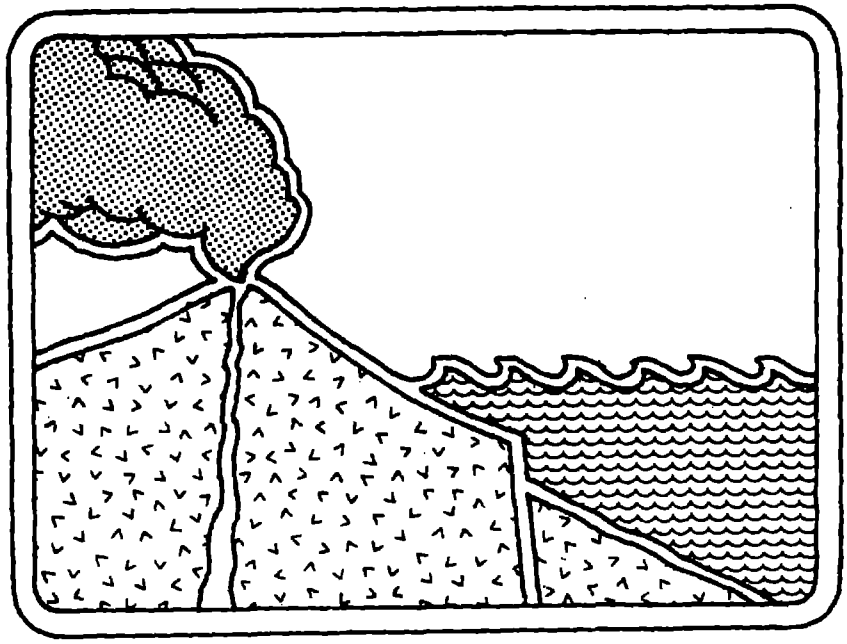

THE 1994 SKAGWAY TSUNAMI TIDE GAGE RECORD

Dennis Nottingham, P.E.
Peratrovich, Nottingham & Drage, Inc.
1506 West 36th Avenue
Anchorage, Alaska 99503

ABSTRACT

The tide gage record from a landslide generated tsunami which occurred November 3, 1994, in Taiya Inlet near Skagway, Alaska has been calibrated.

The initial short-period gage trace does not appear to have been wave generated, but instead in all probability is an instrument reaction to an atmospheric pressure change.

The remainder of the gage trace consists of approximately three-minute period waves starting with an initial drawdown. Waves during the first part of the trace have been calibrated to illustrate actual wave heights.

Introduction

A tsunami wave with a period of approximately three minutes occurred in Taiya Inlet near Skagway, Alaska on November 3, 1994. Various speculations have been suggested as to the cause and location of ground movements large enough to produce the observed and measured sea level variations.

Eyewitnesses vividly described the event and Bruce A. Campbell (1,2) has carefully documented these observations and deduced the timing of the various features that were observed in a rigorous analysis summarized by Mader (3). Mader and Campbell have accurately explained the approximate volume and location of the primary slide, and determined its direction, headward progression, and sea wave characteristics created by it as shown on Figure 1.

A NOAA tide gage located near the event recorded a trace that clearly documents the effects of the event at that specific location. Mader(3) specifically addresses an anomaly in the tide gage recording and properly suggests additional studies are called for to explain the anomaly. The anomaly occurs in the recording during the first minute of the event. The gage trace shows a crest wave occurring with a period much less than the three-minute period of the remaining trace.

The Skagway NOAA tide gage traces from just prior to 7:00 PM on November 3, 1994, were produced by a Metercraft Model 7602 gas-purged pressure recording (Bubbler) tide gage (see Figure 2). The gage bellows and chart were set up to record 30-foot tide ranges using a 28-cubic-inch orifice located at Elevation -10± MLLW.

Peratrovich, Nottingham & Drage, Inc. owns an exact duplicate gage assembly and installed it in conjunction with a 30-foot seawater standpipe for test purposes in 1996. By raising and lowering the gage orifice, tidal conditions similar to those occurring in Skagway could be modeled. Dynamic effects of this test procedure were negligible because of the length of the wave periods involved. Adjustment of the test gage to account for known Skagway sea conditions on November 3, 1994, provided gage calibration which reflected actual conditions. This adjustment was important because the gage trace is dampened and does not depict actual wave heights.

Difficulty was experienced attempting to reproduce the first, very short period crest recorded on the original NOAA trace. An exact duplication of the actual NOAA tide gage trace in this area was never achieved during many testing attempts. The "best-fit" results that could be produced were included by Mader(3) in his analysis. While the "best-fit" test gage traces were very close to Mader's numerical results, the first short-period wave anomaly was apparent and further study of the misfit was needed as recognized by Mader(3).

Physical Modeling

Campbell(1,2) reported and discussed one important clue observed by eyewitnesses. As witnessed, southerly winds around 25 MPH were blowing on November 3, 1994, but suddenly stopped about one or two minutes before the event occurred at the PARN dock. Obviously a change in atmospheric pressure resulted. To determine potential effects of barometric pressure change, the Bubbler tide gage was retested with the gage and orifice completely enclosed in a pressure/vacuum chamber so that pressure changes could be introduced into the testing procedure.

Results

Observation of Figure 2 discloses that, the first significant positive and negative gage traces are nearly coincident and it is thus impossible to distinguish much difference in time. This indicated very rapid pen movement and a seemingly impossible wave trace for known conditions. Mader(3) noted that such a short period trace could not have been caused by the tsunami.

Testing with the gage enclosed in the pressure/vacuum chamber illustrated that a negative air pressure of about two inches of Mercury would cause immediate and rapid pen movement which was similar to the initial trace recorded on the NOAA gage as shown in Figure 3. For reference, historical barometric variation in this region is about three-and-one-half inches of Mercury.

Repeated standpipe testing, with an initial drawdown, reproduced traces similar to previous testing as shown in Figure 3, but without the short period anomaly as confirmed numerically by Mader (3). Additional testing, including vibrations and impact to the gage were performed, but did not produce significant gage trace irregularities.

Superposition of the trace produced during the vacuum test described above and the trace resulting from dampened standpipe tests produced a trace almost exactly as recorded by the NOAA tide gage at Skagway on November 3, 1994, as shown in Figure 5.

It should be noted that Figure 2 discloses the fact that smaller long-period waves occurred about 10 minutes before the tide gage recorded larger waves. These were probably caused by initial sea bottom slides in the inlet remote from the dock, since no distress was reported by eyewitnesses prior to the event.

Conclusion

Further investigation into NOAA tide gage traces at Skagway, Alaska recorded on November 3, 1994, indicates that the recorded trace is most likely a combination of a nearly constant period (three minutes) tsunami waves and very rapid pen trace movement as a result of an almost instantaneous atmospheric pressure change. This

change was caused by the large crest wave and drawdown described by Campbell. It is concluded that the initial, very short period gage trace was not wave generated, but an instrument reaction to an atmospheric pressure change.

References

(1) Bruce Campbell, Report of a Seafloor Instability at Skagway, Alaska – November 3, 1994", Campbell and Associates Report of January 16, 1995.
(2) Bruce Campbell, "Skagway Seafloor Instability Re-Analysis and Update", Campbell and Associates Report of January 28, 1997.
(3) Charles L. Mader, "Modeling the 1994 Skagway Tsunami", Science of Tsunami Hazards, 15, 41-48 (1997).

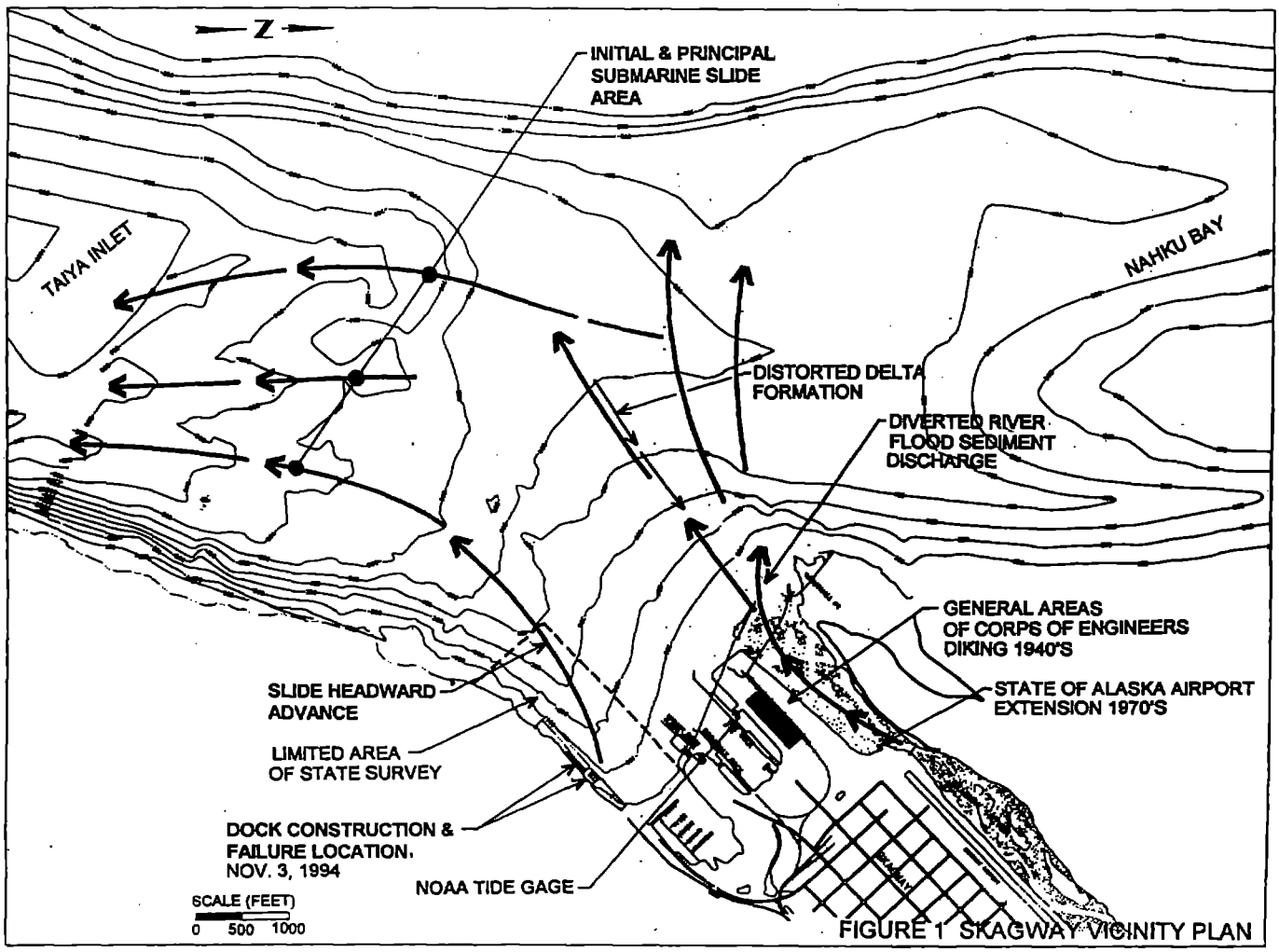

FIGURE 1 SKAGWAY VICINITY PLAN

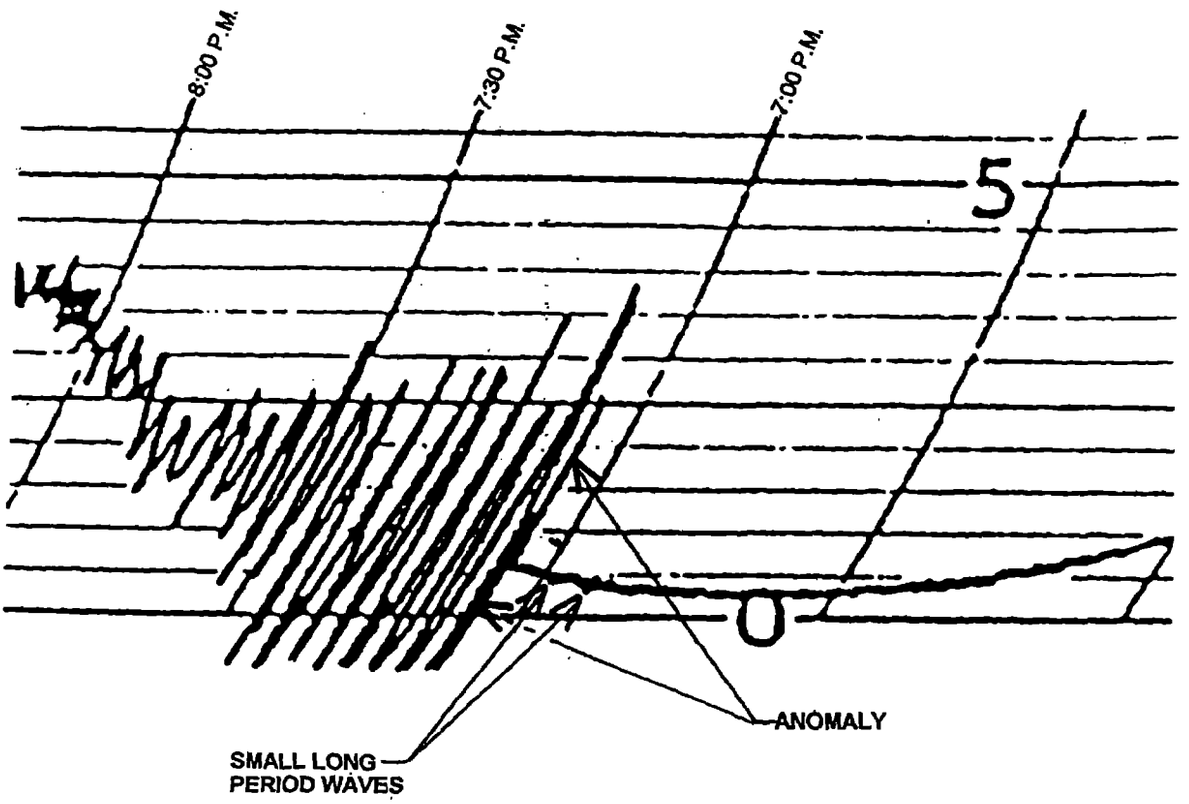

FIGURE 2 NOAA TIDE GAGE TRACE
SKAGWAY, ALASKA
NOVEMBER 3, 1994

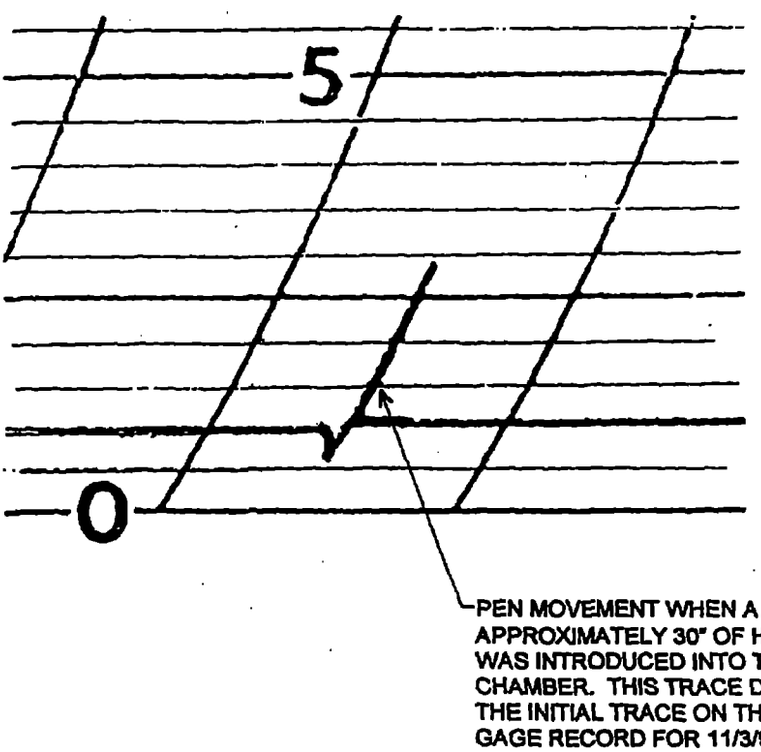

FIGURE 3 TIDE GAGE 30" H_2O (1.1 psi) VACUUM TEST

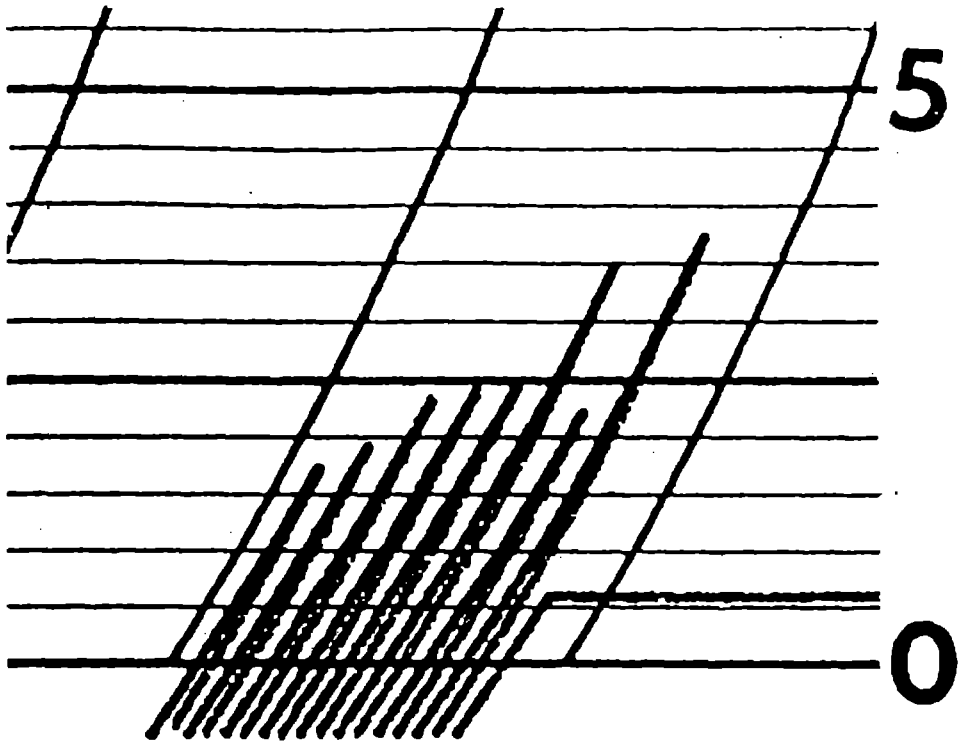

A. REPRODUCED TIDE GAGE TRACE
(NO CHANGE IN ATMOSPHERIC PRESSURE)

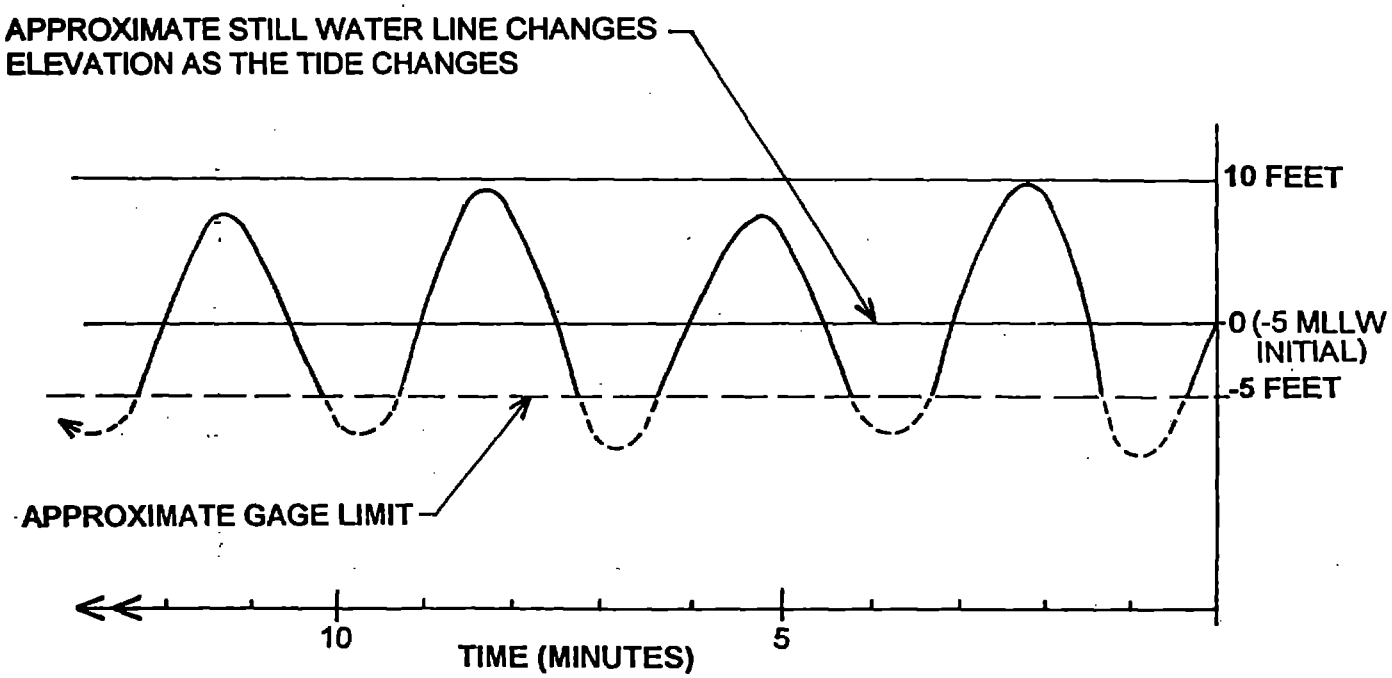

B. ARTIFICIAL WAVE PATTERN CREATED TO REPRODUCE
ACTUAL NOAA TRACE

FIGURE 4 RESULTS OF STANDPIPE-TIDE GAGE TESTS

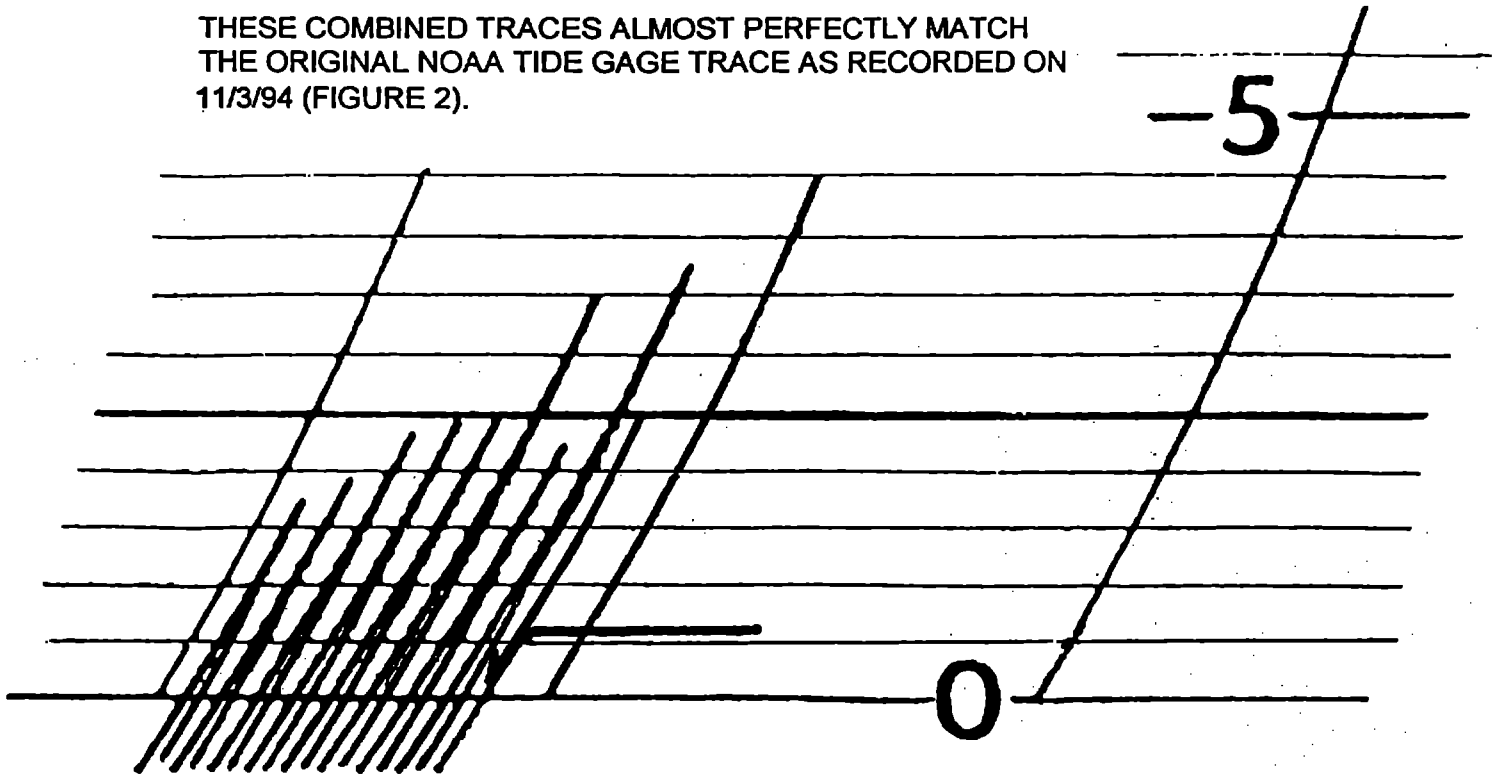

FIGURE 5 SUPERIMPOSED TRACES FROM FIGURES 3 & 4

LANDSLIDE-GENERATED TSUNAMI IN SKAGWAY, ALASKA

Zygmunt Kowalik

Institute of Marine Science
University of Alaska Fairbanks
Fairbanks, AK 99775

ABSTRACT

Landslide on November 3, 1994 produced large-amplitude tsunami in Skagway Harbor. This study uses numerical modeling to investigate generation and propagation of tsunami in the Taiya Inlet and Skagway Harbor. Several mechanisms are invoked to explain persistent motion of a 3 min period, recorded by the tide gage in Skagway Port. It appears that persistent motion was sustained by the resonance transfer of energy between Taiya Inlet and Skagway Harbor due to proximity of periods of the natural oscillations in these domains. Important parameter in the effective transfer of energy from the outside domain to the port is velocity of the landslide. Numerical model used in computations is based on the nonlinear shallow-water equations which are solved by a finite-difference method. Two landslides are studied for investigation of how different source parameters influence tsunami recorded in Skagway Harbor. First, a landslide in proximity to Skagway Harbor is considered and afterwards tsunami generated by a massive landslide in the Taiya Inlet is studied. Numerical experiments indicate that a landslide near Skagway Harbor was unable to sustain tsunami recorded by the tide gage on November 3, 1994.

I. INTRODUCTION.

On November 3, 1994 a large-amplitude tsunami occurred in the Taiya Inlet, Alaska and was recorded by the tide gage in Skagway Harbor (Figure 1). Tsunami wave caused death of one person and damaged Ferry Terminal located on the floating dock. Eye witness report presented by Campbell (1995, 1997) and Mader (1997) describes chronology of events and estimates the wave height to be about 30 ft. This event was analyzed, described and modeled by Kulikov et al. (1996), Raichlen et al. (1996) and Mader (1997). Kulikov et al. (1966) analyzed recorded tsunami by power spectra and detected that the main period of oscillations is close to 3 min. Extraordinary feature of the tidal record is persistence of this short period oscillations for about 30 min. Kulikov et al. (1966) estimated the periods of natural (own) oscillations in the Taiya Inlet and Skagway Harbor and found that both periods are close to 3 min. Thus they postulated resonance exchange of energy between Taiya Inlet and Skagway Harbor. Proposed mechanism for the wave generation is a landslide in proximity to the harbor. Raichlen et al. (1996) also found that the resonance period in Skagway Harbor is close to 3 min. Investigation done by Raichlen et al. (1966) on the property of tide gage installed in Skagway Harbor allows better understanding of the recorded tsunami. Recorded wave has maximum range of about two meters and period approximately 3 min. Calibration of the tide gage made by Raichlen et al. (1996) shows that at the period of about 3 min the signal is damped 40% to 75%. Thus recorded by the tide gage a 2 m wave was, in reality, about two to four times greater. The model utilized by Mader (1997) investigated two slides: a harbor slide and a massive slide in the Taiya Inlet. His results also suggest that the transfer of energy from the massive slide in the Taiya Inlet to the Skagway Harbor oscillations is affected by the landslide velocity. Thus the resonance mechanism suggested by Kulikov et al. (1966) and Raichlen et al. (1966) can be modified by the slide velocity in such a way that the wave energy from the Taiya Inlet is pumped more effectively into the harbor oscillations. The purpose of this paper is to investigate various mechanisms of resonance interactions between the Taiya Inlet and Skagway Harbor. Two different scenarios for the tsunami generation, as proposed by Mader (1997) will be used.

II. MODEL.

The region examined in this study includes upper Taiya Inlet from $59^0 24'$N to $59^0 29'$N and from $135^0 19$W to $135^0 23'$W, Figure 1, upper panel. The depth distribution shown in Figure 1 was compiled by Peratrovich, Nottingham & Drage, Inc. (Campbell, 1995). The datum level is related to the lower low water. Tidal range in the Skagway Harbor is about 8 m, therefore, this range will strongly influence shallow water bathymetry accordingly to the tidal cycle.

The following set of shallow-water equations of motion and continuity is used in the Taiya Inlet domain to describe tsunami generation by a landslide (Kowalik and Murty, 1993, Mader, 1988):

$$\frac{\partial u}{\partial t} + u\frac{\partial u}{\partial x} + v\frac{\partial u}{\partial y} - fv = -g\frac{\partial \zeta}{\partial x} - \frac{rWu}{D}, \tag{1}$$

$$\frac{\partial v}{\partial t} + u\frac{\partial v}{\partial x} + v\frac{\partial v}{\partial y} + fu = -g\frac{\partial \zeta}{\partial y} - \frac{rWv}{D}, \tag{2}$$

$$\frac{\partial \zeta}{\partial t} = \frac{\partial \eta}{\partial t} - \frac{\partial (Du)}{\partial x} - \frac{\partial (Dv)}{\partial y}. \tag{3}$$

Here u and v are the east-west (x) and north-south (y) components of velocity, respectively, g is gravity, f is the Coriolis parameter, ζ is the displacement of the free surface from the equilibrium level, η is the bottom displacement, $H(x,y)$ is the water depth in the equilibrium state, $D = H(x,y) + \zeta + \eta$ is the total depth, $W = \sqrt{u^2 + v^2}$, and r is the bottom friction coefficient.

At all shores, the normal velocity component is assumed to be zero. As for the southern open boundary (Figure 1, top panel), it is assumed that the wave processes occurring inside the numerical domain are not influenced by processes from outside, therefore the radiation condition given by Reid and Bodine (1968) is used.

To construct a numerical scheme, a space staggered grid is applied which requires either sea level or velocity as a boundary condition. The first order scheme is applied in time and in space. The horizontal grids of 22.8 m and of 10 m cover Taiya Inlet. Two different grids are used, so that results from the various grids can be compared. The time step of numerical integration in the coarse grid is 0.1 s and in the fine grid is 0.05 s.

III. INVESTIGATION OF THE OSCILLATORY RESPONSE OF THE SKAGWAY HARBOR TO THE FORCING FUNCTION.

The harbor response to tsunami forcing can be represented as a superposition of the forced and free oscillations. The behavior of the harbor oscillations will depend on the resonance phenomenon (Mei, 1989). Whenever the period of an external force coincides with the free oscillation mode, the resulting motion is amplified. We utilize this phenomenon to investigate natural oscillations of Skagway Harbor. The investigation is done with the help of the basic set (1)–(3) on the 10 m lattice. To induce harbor oscillation through this system of equations, a forcing at the open boundary can be used (Papa, 1977; Kowalik and Murty, 1993). For these experiments a small domain in proximity to the Skagway is considered - Figure 1 (lower panel). At the southern open boundary of this domain a 1 m amplitude periodical sea level oscillation is generated in the range of periods from 25 s to 300 s. At the western and northern open boundaries Reid and Bodine (1968) radiation condition is used so that waves can leave domain without any distortion. To excite harbor oscillations a source of periodical oscillations at the open boundary is applied separately for every period for the duration of about 0.5 h. This duration is usually sufficient for a stationary state to occur in the entire domain. The sea level oscillations recorded in points 1, 2, 3 and 4 (Figure 1, lower panel) is then used for constructing dependence of the amplitude of the signal versus period to locate the maximum in the response function. The summary of investigations for all periodical oscillations in the 25 s to 300 s range is given in Figure 2. The amplitude of oscillations as a function of the period of oscillations at the four points in the Skagway Harbor is depicted.

At the harbor entrance (point 1) the two maxima are observed in the considered range of periods: one close to 100 s and the second around 175 s. In the point 2 the maximum of amplitude occurs at the 171.5 s and at the points 3 and 4 the maximum is located at 168 s. The 168 s period has been defined with an error of $\pm$ 4 s. Waves excited inside the

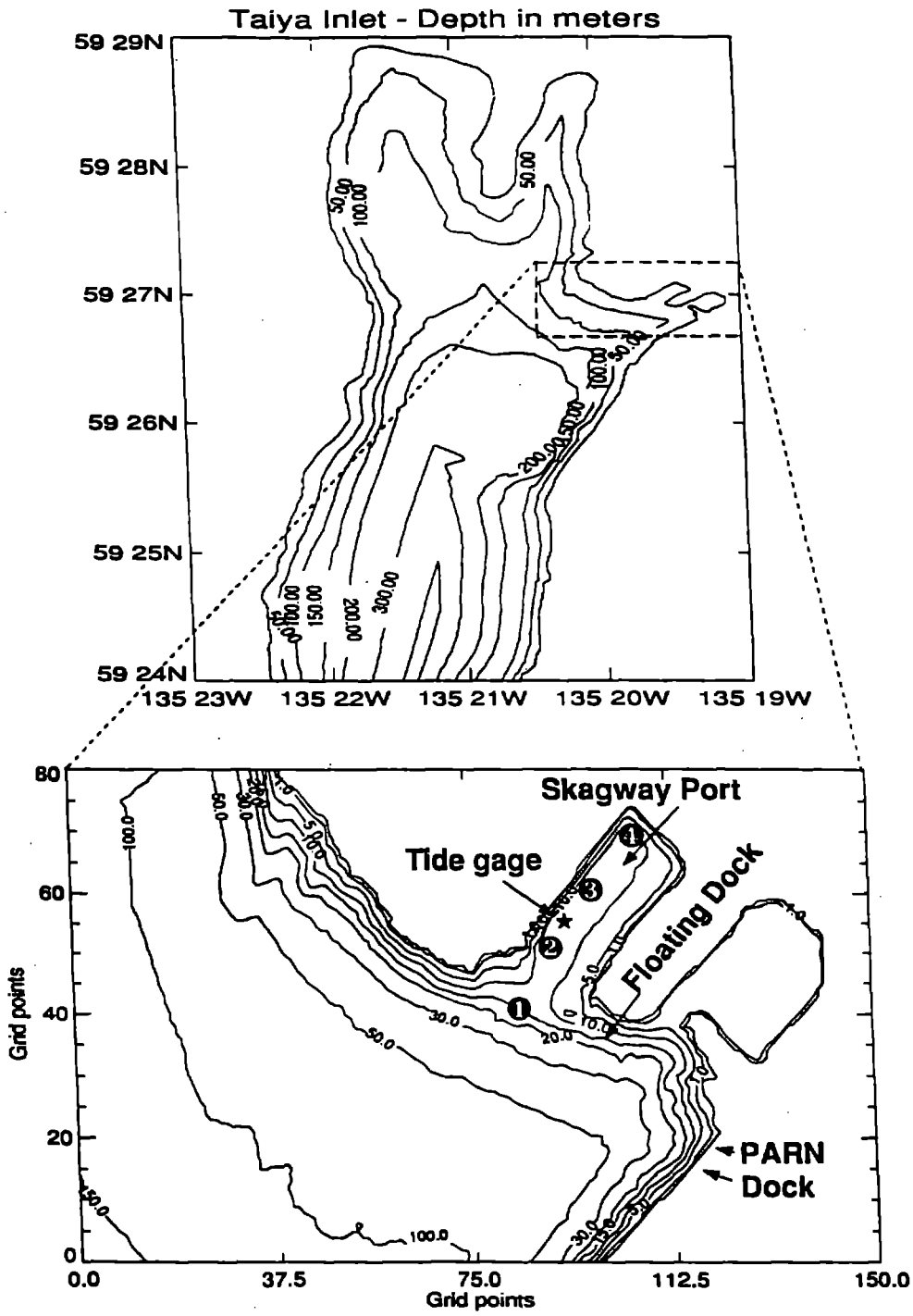

Figure 1. Computational domains and bottom topography. Depth is given in meters. Numbers in the black circles denote locations chosen for the sea level analysis.

harbor by incident oscillations depict strongly enhanced amplitude at the resonance period. The amplitude of oscillations at the 168 s period is 220 cm, 920 cm, 1670 cm and 1900 cm in the points 1, 2, 3 and 4, respectively. Thus the amplification coefficient in the points 2, 3 and 4 relatively to the point 1, is 4.2, 7.6 and 8.6. Therefore, a signal of 168 s period traveling into the harbor is enhanced about 9 times at the end of the harbor. The amplitude of the signal at the 168 s period is growing from the entrance towards the end of the port. We can conclude that the maximum at the 168 s in Figure 2, is related to the lowest mode of the harbor's natural oscillations. This mode of oscillations is generated in an elongated harbor with one open end, therefore the period of this mode is defined as (Kowalik and Murty, 1993):

$$T = \frac{4L}{\sqrt{gh}} \tag{4}$$

Here L is a harbor length, h is an average depth and g is the gravity acceleration. Kulikov et al. (1996) applied above formula to define the lowest mode of natural oscillations in Skagway Harbor and arrived at 191 s period. Thus their result is quite close to the 168 s period we obtained above.

Proximity of a forcing function period to the natural period is a basic condition for the resonance to occur, but our investigations were made under special stipulation, namely the total duration of the oscillations was sufficiently long in time for the steady state to develop. In reality, the tsunami wave is a short and transient signal in time, and usually the time for pumping energy into the resonant (harbor) mode is not sufficient for the steady condition to occur or for the full resonance to develop. In Skagway Harbor the 1994 tsunami event occurred at the time of a low tide of about 1.2 m below lower low water. The depth distribution used to define resonance response curves in Figure 2 is related to the time of the tsunami occurrence. At the different time, the tidal range will influence the shallow water depth needed for computations of the natural oscillation periods.

The above investigations of the natural oscillations in Skagway Harbor we extend to the Taiya Inlet along E-W cross-sections. Since the point of interest is an interaction of the Taiya Inlet oscillations with the natural oscillations in the harbor, only cross-sections close to Skagway Harbor are considered. The natural mode of the oscillation is specified by the following formula,

$$T = \frac{2L}{\sqrt{gh}} \tag{5}$$

Here L is the cross-inlet width and h is the average depth along a cross-section. The largest error in the above formula is caused by the average depth assumption. To diminish this error the depth distribution defined on the 10 m lattice can be used. Moreover, instead of the above averaged formula we apply summation (or integration) along E-W cross-sections accordingly to the formula,

$$T = 2\int_0^L \frac{dx}{\sqrt{gh}} \tag{6}$$

From (6) the period of the basic mode of cross-inlet oscillations is found to be in the range from 145 s to 156 s. This period differs more than 12 s from the resonance period of Skagway Harbor. The average speed of the long gravity waves $c = \sqrt{gh}$ defined on the 10 m numerical lattice is close to 30 m/s.

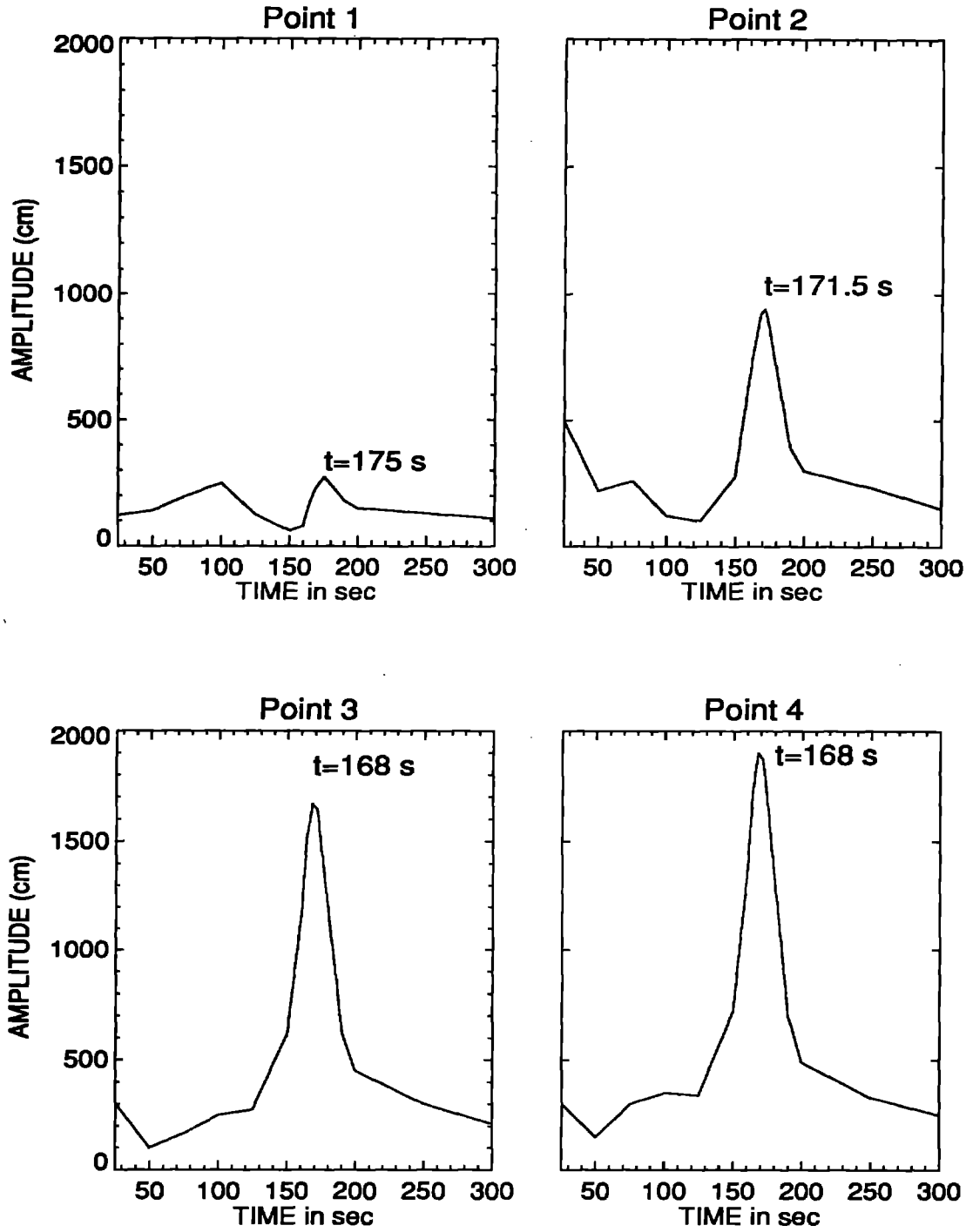

Figure 2. Computed response functions for amplitude in the Skagway Port at four locations shown in Figure1. Response functions are due to the 1 m sea level forcing at the open boundary.

IV. TRANSFER OF ENERGY TO THE HARBOR OSCILLATIONS THROUGH THE SUBMARINE LANDSLIDE.

The mechanism for tsunami generation is based on the transfer of energy from the bottom displacement to the water. Numerous historical records gathered by Lander and Lockridge (1989) demonstrate the generation of very large water waves by landslides. Various mechanisms of transferring energy from the landslide to tsunami waves have been tested through analytical solutions as well as through hydraulic and numerical modeling (Aida, 1969; Imamura and Imteaz, 1995; Kajiura, 1963; Kienle et al., 1987; LeBlond and Jones, 1995; Noda, 1970; Wiegel, 1955).

The Skagway tsunami source model is constructed using the technique of the moving rigid bottom deformation. This motion is transmitted into the water column through the continuity of volume. Two scenarios of tsunami generation have been investigated. In the first, the underwater slide is assumed to enter the Taiya Inlet close to the Pacific and Arctic Railway and Navigation Company (PARN) dock. In the second scenario, the slide occurs in the upper Taiya Inlet with the slide volume of about 21.5 million cubic yards (Mader, 1997). The occurrence of the major slides in the fjords was documented by Bjerrum (1971). He also noted that the time of a slide phenomenon is often associated with the low tides occurrence. Karlsrud and Edgers (1980) analyzed various slides and found that slides may propagate with the velocity larger than 25 m/s. Kienle et al. (1996) investigated tsunami generated by underwater slides and described dependence of the tsunami amplitude on the slide velocity. Proximity of the slide velocity to the phase velocity of the long waves seems to cause enhancement of the tsunami signal. This observation was corroborated by Mader (1997) computation. He established that the transfer of energy from the Taiya Inlet slide to the harbor oscillations is a function of the slide velocity.

Dock Slide

In the first numerical experiment a slide in proximity to the PARN Dock is chosen as a source for the tsunami generation. Here we take extreme slide volume, as suggested by Mader (1997). The slide geometry incorporates two regions of 226 m by 226 m, each - Figure 3, lower panel. In the first region located along the PARN Dock, the bottom was lowered 30 m. In the second region, located seaward from the PARN Dock, the bottom was uplifted 30 m.

Taiya Inlet Slide

The geometry of the massive underwater slide proposed by Campbell (1997) and Mader (1997) for the Taiya Inlet is depicted in the upper panel in Figure 3. The slide moves in increments from North to South until final geometry, depicted in the above figure, is established. Numbers given in Figure 3 for the bottom uplift and subsidence are expressed in meters.

In the first experiment, carried out with the 22.8 m resolution, the PARN Dock instantaneous slide generates tsunami. The model was run for 0.5 h of the process time with the computational time step of 0.1 s. For the first 1000 s of the process the sea level computed in Skagway Harbor at the tide gage location is shown in the Figure 4, upper panel. The sea level spectra calculated from this data is depicted in the Figure 4, lower

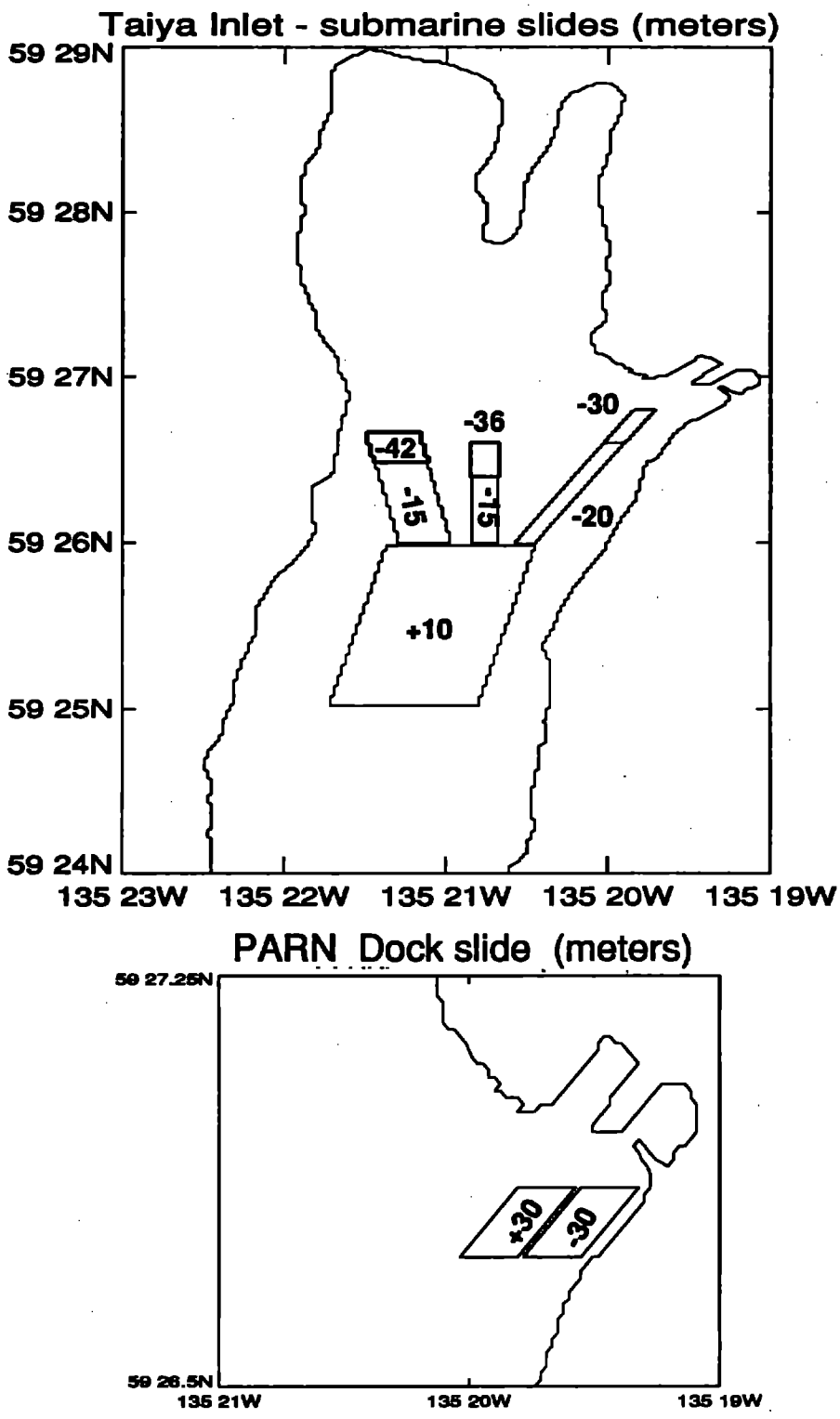

Figure 3. Tsunami source models. Upper panel: massive submarine landslide in the Taiya Inlet. Bottom panel: submarine landslide at the PARN Dock. Bottom uplift and subsidence are given in meters.

panel. The amplitude of the computed tsunami is very small (less than 2 m) and the main peak in the sea level spectra does not correspond to a 3 min period but to a 2 min period. Also, a strong peak at the period of 40 s is present. Moreover, the oscillations occur only for about 10 min and are not sustained for the longer time span. It occurs that the dock slide is unable to transfer energy into the harbor oscillations either due to the short–time occurrence of this slide or due to difference in the periods of slide oscillations and harbor oscillations.

Experiments carried out with an instantaneous massive underwater slide (Figure 3, upper panel) generate different sea level variations at the tide gage location (Figure 5, upper panel). Not only the sea level amplitude becomes bigger but the process of energy transfer into the harbor mode (168 s) takes place as well. The harbor mode becomes dominant in the amplitude spectra (Figure 5, lower panel). In the transfer process an important role plays the second largest peak in the amplitude spectra, of about 2.5 min period. This peak represents lowest mode of the cross-inlet natural oscillations. The area of the cross-inlet oscillation peak partly overlaps with the harbor oscillation peak, making feasible transfer of energy between these two modes.

A set of experiments was carried out to study the influence of the velocity of the massive bottom slide on the tsunami amplitude. The advance of the underwater slide along the inlet's floor is simulated as a progressive uplift or subsidence of the sea floor, propagating from the North to the South at a speed ranging from 5 m/s to 115 m/s. The amplitude response at the 168 s period to the various slide velocities was investigated at the tide gage location in Skagway Harbor (Figure 6). The maximum amplification of the amplitude occurs at the slide velocity of 35 m/s. This amplitude is approximately two times larger than the amplitude generated by an instantaneous uplift and subsidence. One can also assume that this enhancement depends on the slide geometry as well. The enhancement of tsunami amplitude through the slide velocity is probably related to the average velocity of tsunami propagation, which in the Taiya Inlet, is close to 30 m/s. It seems that closeness of the slide velocity and the tsunami propagation velocity is important condition for the effective energy transfer from the slide to the tsunami.

In the Figure 7, the sea level and amplitude spectra are given at the tide gage location for the massive slide moving with velocity of about 32.7 m/s. The sea level and the amplitude spectra is different from the sea level generated by an instantaneous bottom change depicted in Figure 5. The sea level shows slowly decaying in time the 3-min oscillations. The amplitude spectra unfolds the physics of this phenomenon. Due to the slide velocity the energy from the slide is pumped very effectively into the harbor mode. The cross-sectional oscillations of 2.5 min period are also present, because of the small amplitude they play secondary role in the exchange process. Above results are obtained by the model with the horizontal space resolution of 22.8 m. To verify result from this grid a higher horizontal resolution of 10 m is used. In Figure 8 the results for the slide velocity of about 40 m/s obtained in the both numerical lattices are shown. Temporal changes of the sea level and sea level spectra are quite similar. The fine grid resolves shorter waves and therefore more energy in this grid is directed to the shorter periods. To arrive to the actual sea level changes a comparison of the computed sea level against sea level recorded by the tide gage requires calibration of the tide gage record. Here, a few periods of oscillations from the onset of tsunami are considered. We use calibration made by Raichlen et al. (1996) and especially

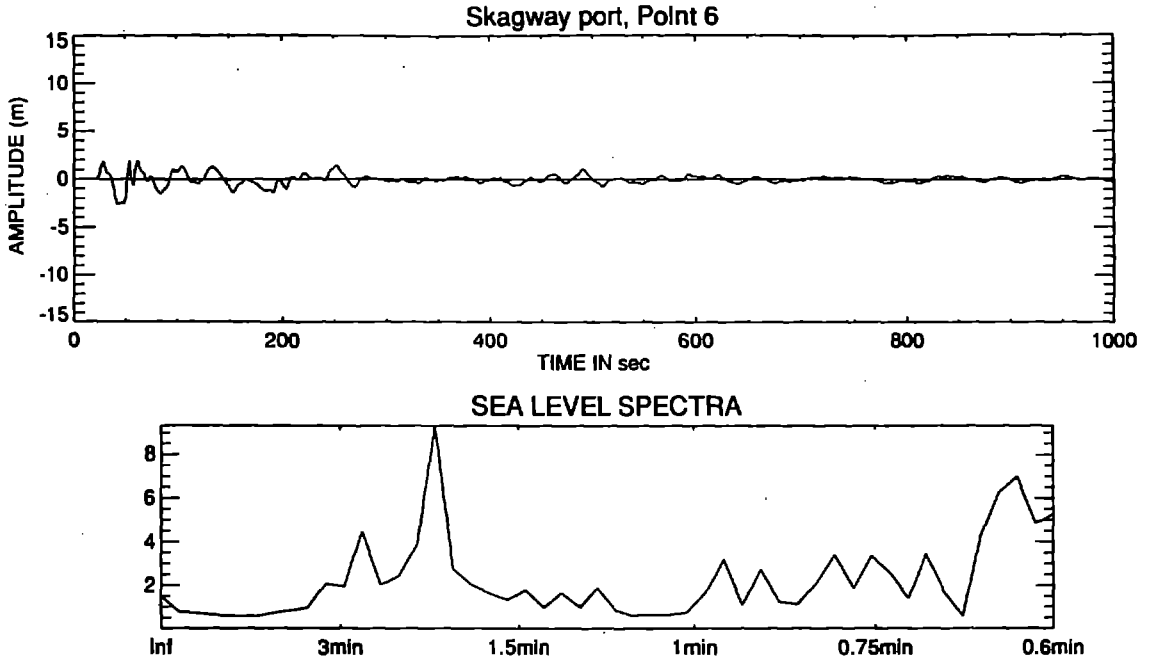

Figure 4. Upper panel: Sea level at the tide gage location. Bottom panel: Sea level spectra. Tsunami source: Instantaneous slide at the PARN Dock.

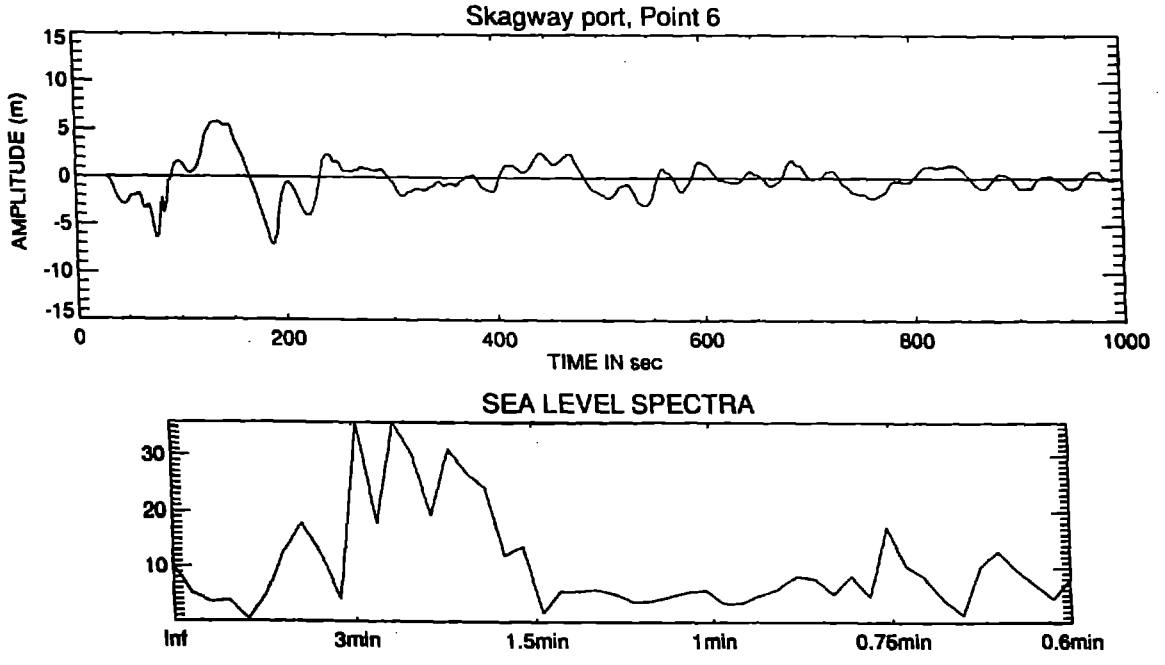

Figure 5. Upper panel: Sea level at the tide gage location. Bottom panel: Sea level spectra. Tsunami source: Instantaneous massive slide in the Taiya Inlet.

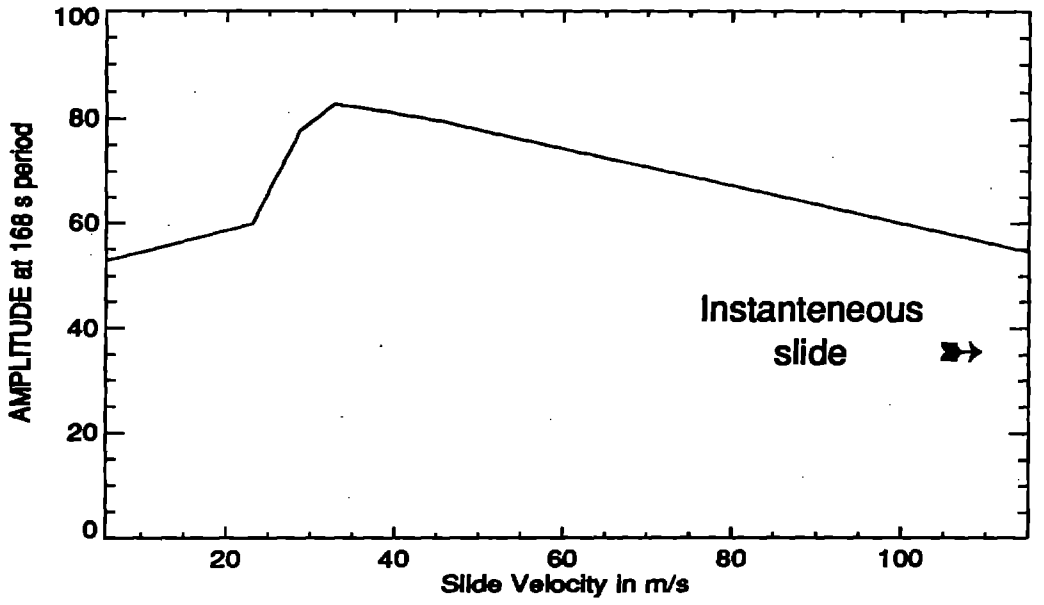

Figure 6. Computed response function for amplitude at the 168 s period. Response function is due to massive landslide. Velocity of the landslide is changing from 5 m/s to 115 m/s.

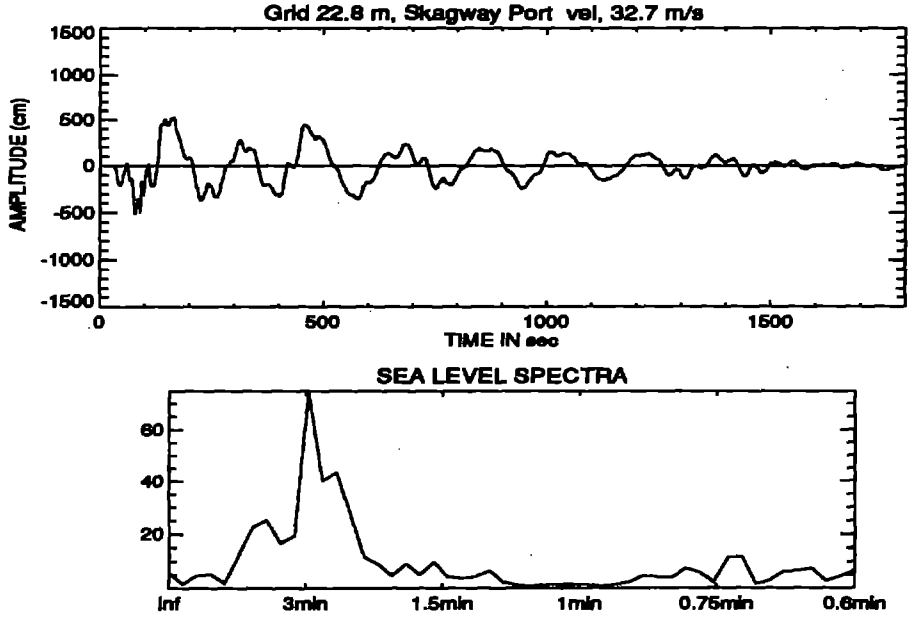

Figure 7. Upper panel: Sea level at the tide gage location. Bottom panel: Sea level spectra. Tsunami source: massive slide moving with velocity 32.7 m/s.

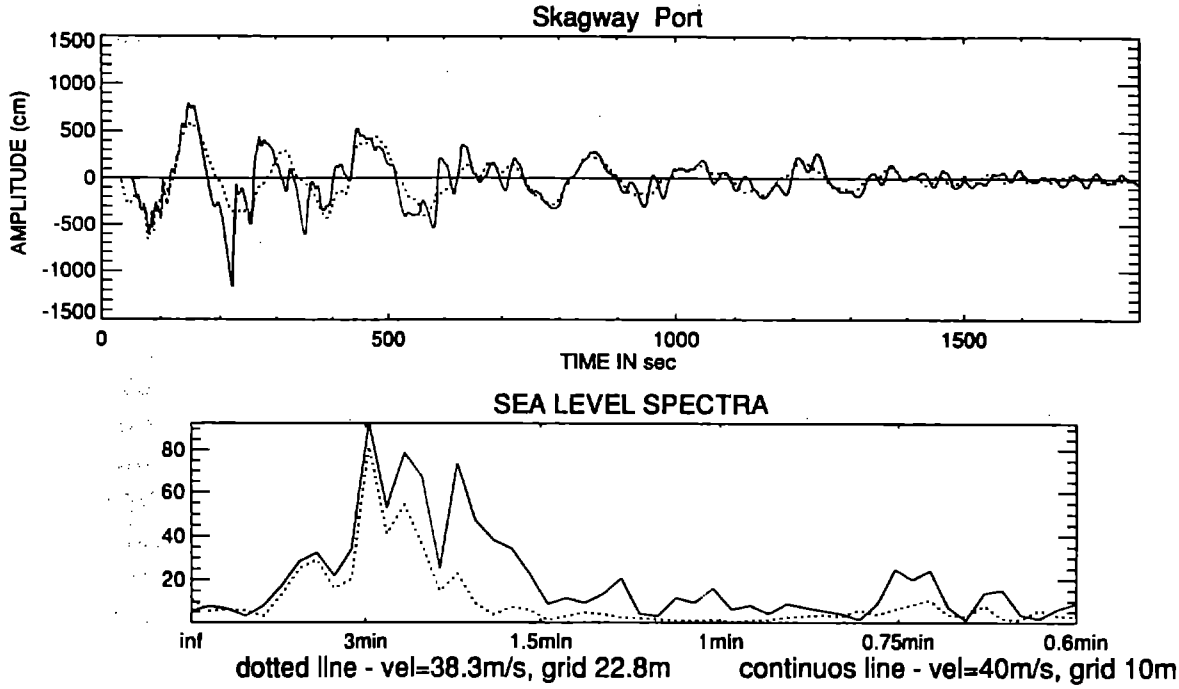

Figure 8. Upper panel: Sea level at the tide gage location. Bottom panel: Sea level spectra. Continuous line: slide velocity 38.3 m/s and computational grid equals to 22.8 m. Dot line: slide velocity 40 m/s and computational grid equals to 10 m.

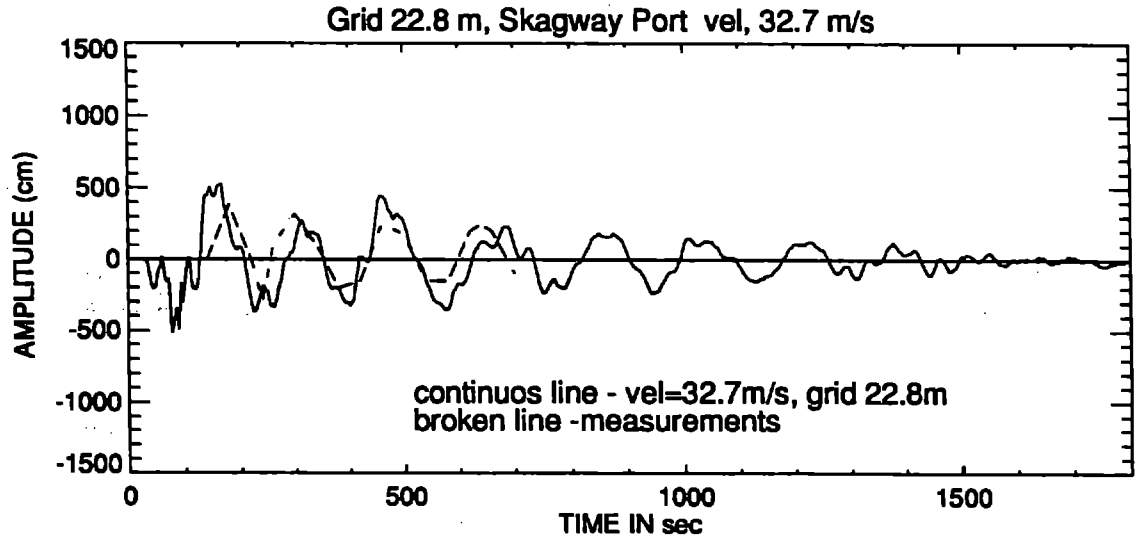

Figure 9. Sea level at the tide gage location. Continuous line denotes result obtained from computations. Broken line depicts measurement corrected for the tide gage dumping.

careful calibration of the initial oscillations made by Peratrovich, Nottingham & Drage, Inc. (Campbell, 1995; Nottingham, 1997). As shown in Figure 9 the computed elevations turned out to be in satisfactory agreement with those obtained from observation.

V. MOTION OF THE FLOATING DOCK.

The Floating Dock was located in the harbor at the end of a jetty (Figure 1, lower panel) and it served as Ferry Terminal. Tsunami caused about one million dollars damage to the Floating Dock, but replacement of the dock, as estimated by Lander (1995), may co st twenty million dollars. The Floating Dock was moored with thirteen chains, thus allowing movement of the dock on tidal wave. During tsunami event all chains were broken and the dock was moved west from the original locations. Complicated movement of the dock during tsunami event was described by the Raichlen et al. (1996). To identify water movement at the dock location we use results of two simulations of tsunami event generated by the PARN Dock slide and massive Taiya Inlet slide. In these computations a 22.8 m grid is applied. A number of the water particles is released at the dock location and their movement is monitored in time. Since the particle trajectory is specified by the Lagrangian velocity we use definition of this magnitude given by Longuet-Higgins (1969) as superposition of Eulerian and Stokes velocity

$$\vec{u}_L = \vec{u}_E + \vec{u}_S \tag{7}$$

The change in the position of specific particle in the horizontal plane is composed by the two terms as well

$$dx = udt + 0.5(u\frac{\partial u}{\partial x} + v\frac{\partial u}{\partial y})(dt)^2 \tag{8a}$$

$$dy = vdt + 0.5(u\frac{\partial v}{\partial x} + v\frac{\partial v}{\partial y})(dt)^2 \tag{8b}$$

Above formulas are used to compute particle trajectories. For tsunami generated by the PARN dock slide a group of six particles was tracked and their trajectories are shown in Figure 10. Within the first 50 s of process the particles covered the main portion of the traveled distance. The remaining trajectory is a decaying circular motion around a stationary position. For quick estimate of the distances traveled by the particles in this figure the 22.8 m lattice has been depicted.

In the second experiment the motion of the Ferry Terminal Dock caused by an instantaneous massive slide in the Taiya Inlet has been studied. Trajectories of the three particles are given in the Figure 11. Strong motion occurs both to the east and west from the initial locations. This study case better explains movement to the west of the Ferry Terminal Dock during tsunami event.

VI. DISCUSSION AND CONCLUSIONS.

Rigid bottom deformation, conservation of the landslide volume and continuity of the movement between the landslide and the fluid are important assumptions for the theories

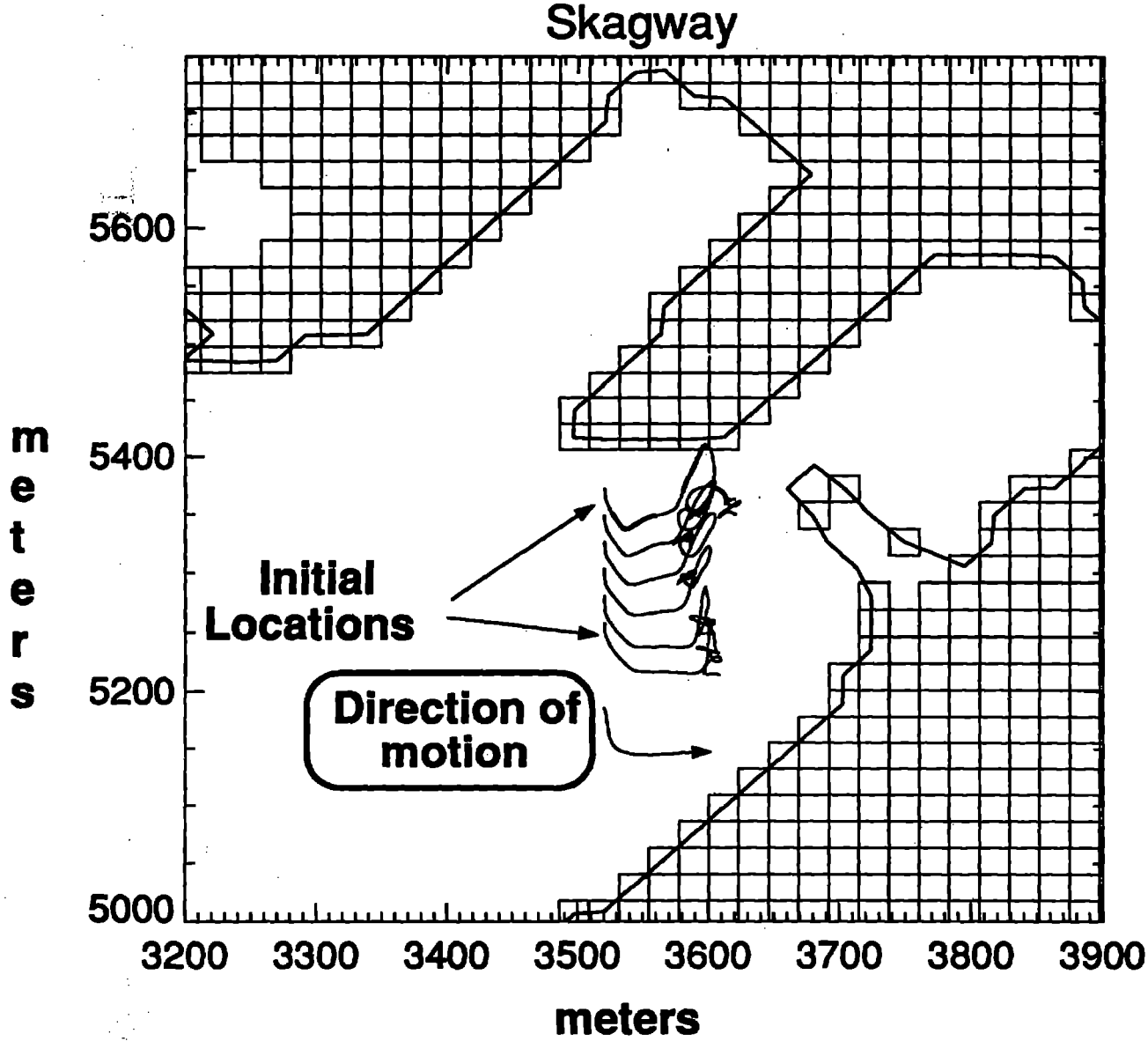

Figure 10. PARN Dock instantaneous slide. Computed trajectories of the water particles during initial 3-min period. Lattice depicts a numerical grid with the grid-distance of 22.8 m.

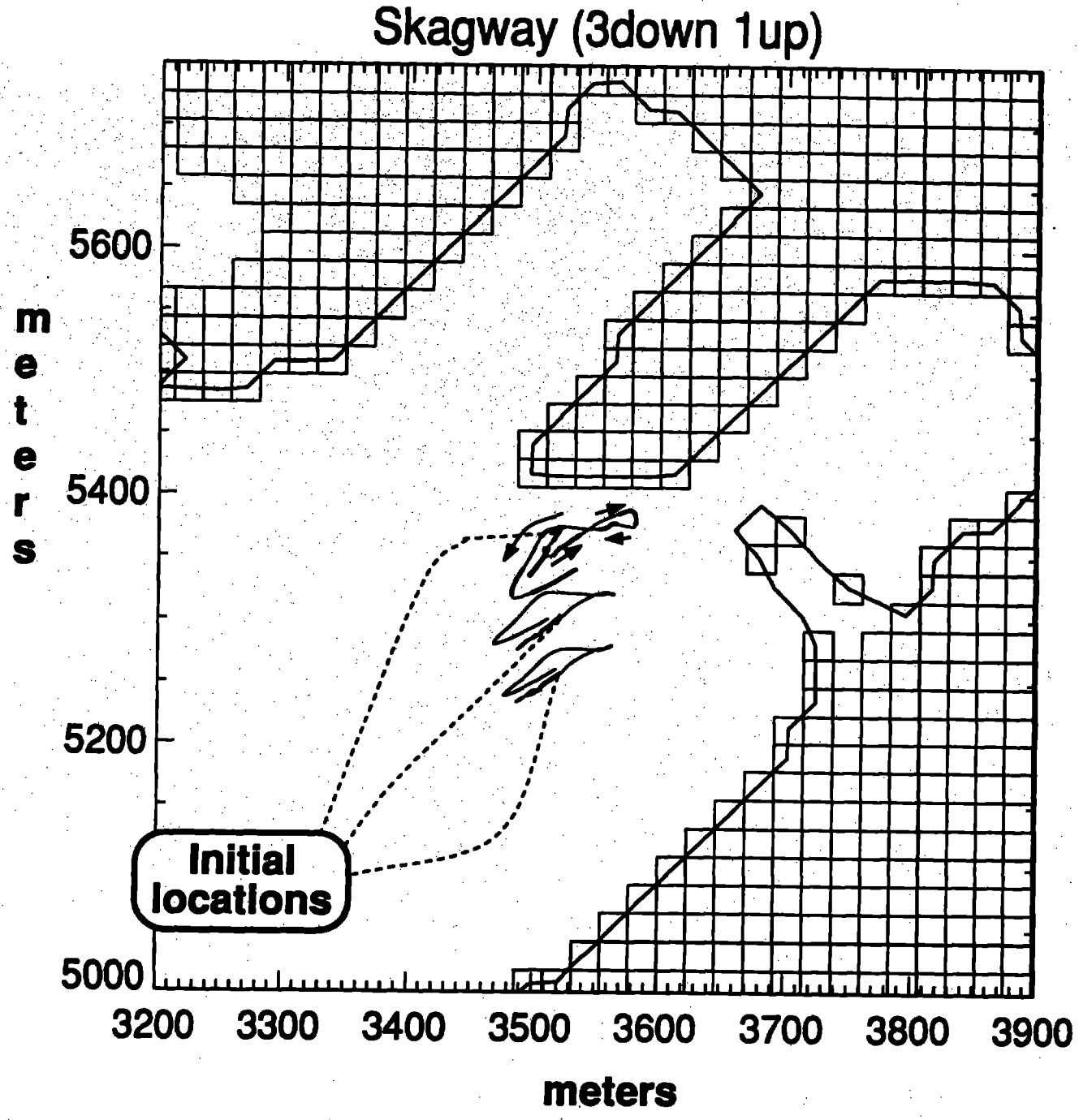

Figure 11. Instantaneous slide in the Taiya Inlet. Computed trajectories of the water particles during initial 3-min period. Lattice depicts a numerical grid with the grid-distance of 22.8 m.

of the wave generation by a landslide. As LeBlond and Jones (1995) pointed out, these assumptions probably generate an overestimated source function. Typically, a landslide is composed of unconsolidated sediments which move downslope and are accumulated at a new location. The interaction of the unconsolidated sediments is not always a volume conserving process.

Wiegel's (1955) experiments also show that the waves produced by sliding deformable material are smaller than those produced by undeformable materials. Therefore, the calculations performed in this study, which take instantaneous uplifts of the sea floor for the initial conditions, must be upper bounds on the size of the tsunami waves generated by the Taiya Inlet slide.

Temporal changes of the tsunami wave amplitude at the tide gage location in Skagway Harbor was studied to identify the cause of persistent short-period oscillations. For this purpose we investigated the natural oscillations inside Skagway Harbor and found that the main period is equal to 168 s and the gravest modes of the Taiya Inlet cross-section oscillations is close to 2.5 min. These two periods are quite close, therefore, energy from the Taiya Inlet oscillations can be pumped into the harbor oscillations. It occurs that this mechanism, though important, is not very effective. A series of experiments was undertaken to assess dependence of the tsunami wave amplitude on the velocity-time history of the landslide. The slide velocity seems to be an additional mechanism required for the effective pumping of wave energy into the harbor mode of oscillation. The moving landslide in comparison to an instantaneous bottom deformation, offers a longer duration time for the energy pumping into the harbor oscillations. The most effective transfer of energy from the moving landslide to the water waves takes place when the landslide velocity matches the tsunami propagation velocity. In the Taiya Inlet the tsunami propagation velocity is close to 30 m/s, while the strongest tsunami is generated by a landslide velocity of 35 m/s.

The results of the computations simulate the tsunami recorded by the tide gage in Skagway Harbor rather well, suggesting that the numerical model presented here describes the processes of generation and propagation adequately.

ACKNOWLEDGMENTS

I am grateful to Dr. Charles Mader for his cooperation, help and discussions. Staff from Peratrovich, Nottingham & Drage, Inc., Anchorage, Alaska was most helpful in sharing bathymetry and calibrated sea level data. My sincere thanks to Dr. Alexander Rabinovich for discussions on resonance phenomena in the Skagway Harbor and Taiya Inlet.

REFERENCES

Aida, I. 1969. Numerical experiments for tsunamis caused by moving deformations of the sea bottom. *Bull. Earthq. Res. Inst. Tokyo Univ.*, **47**(1): 849–862.

Bjerrum, L. 1971. Sub-aqueous slope failures in Norwegian fjords. Publ. 88, Norw. Geotech. Inst., Oslo, 8pp.

Campbell, B. 1995. *Report of a Seafloor Instability at Skagway, Alaska – November 3, 1994*, Campbell and Associates Report of Jan. 16, 1995, Anchorage, Alaska.

Campbell, B. 1997. *Skagway Seafloor Instability Re-Analysis and Update*, Campbell and Associates Report of Jan. 28, 1997, Anchorage, Alaska.

Imamura, F. and M. Imteaz. 1995. Long waves in two layers: governing equations and numerical model. *Science of Tsunami Hazard*, **11**(1): 3–24.

Kajiura, K. 1963. The leading wave of tsunami. *Bull. Earthq. Res. Inst. Tokyo Univ.*, **41**(3): 535–571.

Karlsrud, K. and L. Edgers. 1980. Some aspects of submarine slope stability. In *Marine Slides and Other Mass Movements*, Plenum, New York, 61–81.

Kienle, J., Z. Kowalik and T.S. Murty. 1987. Tsunami generated by eruptions from Mount St. Augustine Volcano, Alaska. *Science*, **356**: 1442–1447.

Kienle, J., Z. Kowalik and E. Troshina. 1996. Propagation and runup of tsunami waves generated by Mt. St. Augustine Volcano, Alaska. Science of Tsunami Hazards, **14**, 3: 191–206.

Kowalik, Z. and T.S. Murty. 1993. *Numerical Modeling of Ocean Dynamics*. Advanced Series on Ocean Engineering, Volume 5. World Scientific Publ., 481 pp.

Kulikov, E. A., A. B. Rabinovich, R. E. Thomson and B. D. Bornhold. 1996. The landslide tsunami of November 3, 1994, Skagway Harbor, Alaska. *Journal of Geophysical Research*, **101**, 6609–6615.

Lander, J. F. 1995. Nonseismic tsunami event in Skagway, Alaska. *Tsunami Newsletter*, **1**, 8–9.

Lander, J. F. and P. A. Lockridge. 1989. *United States Tsunamis*. National Geoph. Data Center. Boulder, 265 pp.

Longuet-Higins, M. S. 1969. On the transport of mass by the time-varying ocean currents. *Deep Sea Res.*, **16**, 431–447.

LeBlond, P.H. and A.T. Jones. 1995. Underwater landslides ineffective at tsunami generation. *Science of Tsunami Hazard*, **11**(1): 25–26.

Mader, L.Ch. 1988. *Numerical modeling of water waves*. Berkeley: University of California Press.

Mader, L. Ch. 1997. Modeling of the 1994 Skagway tsunami. *Science of Tsunami Hazard*, **15**(1): 41–48.

Mei, Ch. C. 1989. *The Applied Dynamics of Ocean Surface Waves.* World Scientific, Singapore, 740pp.

Noda, E. 1970. Water waves generated by landslides. *J. of Waterways, Harbors and Coastal Engineering Division*, Proc. Am. Soc. Civ. Eng., WW4: 835–853.

Nottingham, D. 1997. The 1994 Skagway tsunami tide gage record. Manuscript submitted to *Science of Tsunami Hazard.*

Papa, L. 1977. The free oscillations of the Ligurian Sea computed by H–N Method. *Deutsche Hydrographische Zeitschrift*, **30**, 81–90.

Raichlen, F., J. J. Lee, C. Petroff and P. Watt. 1996. The generation of waves by a landslide: Skagway, Alaska – a case study. Proceedings of 25th International Conference on Coastal Engineering, Orlando, Florida, 14pp.

Reid, R.O. and R.O. Bodine. 1968. Numerical model for storm surges in Galveston Bay. *J. Waterway Harbor Div.*, **94(WWI)**, 33–57.

Wiegel, R.L. 1955. Laboratory studies of gravity waves generated by the movement of a submerged body. *EOS*, **36**: 759–774.

The January 1, 1996 Sulawesi Island Tsunami

Efim Pelinovsky
Institute of Applied Physics, Russian Academy of Sciences,
46 Uljanov St., Nizhny Novgorod, 603600, Russia
Email: enpeli@appl.sci-nnov.ru

Dede Yuliadi
Navy Hydro-Oceanographic Service, Jakarta, Indonesia

Gegar Prasetya and Rahman Hidayat
Tsunami Research Center - Coastal Engineering Laboratory,
Agency for the Assessment and Application of Technology, Jakarta, Indonesia

Abstract

On January 1, 1996 at 16:05 p.m. local time an earthquake of magnitude M=7.8 struck the central part of Sulawesi Island (Indonesia). It was accompanied by tsunami waves 2 - 4 m high. 9 people were killed and 63 were injured. A tsunami survey was conducted by Indonesian and Russian specialists. The measured tsunami runup heights and eyewitness accounts are reported and discussed. Historical data on the Sulawesi Island tsunamis are analysed. Tsunami risk prediction in the central part of Sulawesi Island has first been carried out.

1. Introduction

On January 1, 1996 at 16:05 p.m. local time (8:05 a.m. GMT) a strong earthquake struck the central part of the Sulawesi Island, Indonesia, approximately 180 km north of the Palu town (Figure 1). The Indonesian Meteorological and Geophysical Agency estimated the earthquake magnitude to be $M = 7$ on the open Richter scale, the location of the epicenter is in the Makassar Strait at 0.60^0N and 119.92^0E, 39 km deep. In the villages closest to the epicenter, the earthquake intensity was 6 on the Modified Mercalli Intensity Scale (MMI). According to official reports, in the Tonggolobibi village 9 people were killed and 63 were injured by a 2 m high tsunami, more than 400 houses were destroyed and became unfit for living. The tsunami was of a local character and the hit area was an approximately 100-km-long coastline. The Pacific Tsunami Warning System estimated the earthquake magnitude to be 7.7, its location at 0^0N., 120^0E, and did not declare tsunami warning in the Pacific. No data on tsunami waves out of Sulawesi Island were instrumentally recorded.
In accordance with modern practice an international team was organized with two specialists from Indonesia and one from Russia to conduct quantitative survey of the tsunami characteristics and tsunami hazard analysis in that region. Three weeks after the earthquake and tsunami the team began its survey gathering field data from January 21 through January 30, 1996. The methods of tsunami wave height measurements and residence inquiries were the same as in other international tsunami surveys, (see, for example, Choi et al., 1994; Yeh et al., 1995); these methods are recommended by the IUGG International Tsunami Commission. The measured tsunami runup heights and eyewitness accounts are presented in this paper. Historical data on tsunamis in that region are discussed and the tsunami risk in the central part of Sulawesi Island is predicted.

2. Historical tsunami data

Recently tsunamis occur in Indonesia almost every year since 1992: Flores Island (December 12, 1992, runup height was 20 m, 2000 people were killed) (Yeh et al., 1993), Java Island (June 2, 1994, wave height equalled about 13 m, 200 people were killed, a tsunami of about 4 m high was observed in Australia) (Foley, 1994), the east part of Timor Island (May 14, 1995, the wave height was 4 m, 8 people were killed) (Prasetya and Jumadi, 1995) and, finally, the present event of January 1, 1996 on Sulawesi Island[1]. The majority of these events have been investigated by International teams and promoted the elaboration of unified requirements and methods for tsunami data analysis.
Tsunamis frequently struck Sulawesi Island. According to catalogs (Soloviev and Go, 1984; Soloviev, Go, Kim, 1992) a total of 14 tsunami cases were recorded on Sulawesi Island within 1820 - 1982, i.e. one tsunami each 11 years. We would mention four destructive tsunamis of this century which occurred in the central part of Sulawesi Island where the present tsunami took place. Their parameters are given in Table 1 (all dates are GMT) and the epicenters of the earthquakes are shown in Fig. 2. Of interest is a very strong tsunami with a runup height up to 15 m generated within a relatively weak seismic event (of magnitude 6.3) in 1927, but the origins referred to in the catalog cannot be verified now. It should be stressed that the epicenters of all those earthquakes are located practically near the coastline.

Table 1

Characteristics of earthquakes and tsunamis in the central part of Sulawesi Island

Year	Date	Latitude	Longitude E	magnitude M	Wave height (m)
1927	01.12	0.7^0S	119.7^0	6.3	15
1938	19.05	1^0S	120^0	7.6	3
1968	14.08	0.2^0N	119.8^0	7.4	10
1996	01.01	0.83^0N	120.01^0	7.7	3.4

We shall give a brief description of those events taken from catalogs.
1927, December 1, 12:37 p.m. (4:37 a.m. GMT). There was a strong earthquake with source in the region of Palu Bay[2]. At Palu, three large stalls collapsed completely at the market. All the remaining structures suffered some damage. The main road, leading to the corn market, was heavily damaged, and some side streets behind

[1] Note that on February 17 one more eartquake and tsunami attacked Irian Java, Indonesia, 110 eople were killed. The tsunami wave had a height of 7.7 m and it reached Japan, where waves up to 1 m ere recorded.
[2] The majority of the geographical names from this section are presented in Figure 2.

the bazaar subsided about 50 cm. At Borowaru, market stalls were completely destroyed and the building of the district administration was heavily damaged. At Donggala, the gallery of the office of the local official partly collapsed. The earthquake was felt clearly all over the west of the middle part of Sulawesi Island. The maximal radius of perceptibility was 230 km. At the same time, a tidal wave appeared in Palu Bay. It lasted 30 seconds and had a height of 15 m. The wave destroyed huts in the shore zone; 14 people died and 30 were injured. At Talise, a pier with a ladder was completely washed away. The sea became 12 m deeper. Subsequent shocks of the earthquake were felt on December 1, 2, 3, 5 and 17 at Parigi, Malitou, Palu and Talise.

1938, May 20, 1:00 a.m. (May 19, 17:08 p.m. GMT). There was a destructive earthquake with source in Tomini Bay[3]. It was felt almost all over Sulawesi Island and on the east of Kalimantan Island. It reached its greatest force in the region of Parigi. Here 942 homes (more than 50%) collapsed in 34 villages and 184 homes were damaged. In Pelawa settlement, trees were uprooted. At the settlement of Marantale, the ground cracked and split in the coconut plantation; one home and the surrounding banana plantations shifted 25 m. The roads were covered with numerous cracks up to tens of metres long and 50 cm wide; here and there, mud flowed out of them; some plots of ground subsided. At Parigi, the school and the kirk collapsed; most wood, concrete and brick structures did not suffer. In the region of Palu and Donggala, the damage was slight, and in the regions of Poso and Tinombo, there no damage at all, despite the strong tremors. There were many aftershocks.

Following the earthquake, a tidal wave 2 - 3 m high, according to some sources, surged onto the coast of the bay from about Toribulu to Parigi. At Toribulu, the sea suddenly retreated 80 m and then returned with force. Between Lemo and Makatate, 14 villages suffered from the wave. In places, the water encroached 40 - 80 m inland. Seventeen people drowned, one at Ampibabo and the rest at Parigi. At Parigi, a pier was washed away, and warehouses and navigation signals were damaged. many cattle and coconuts were washed away. It was reported that oscillations in sea level with a range of 8 cm were registered by the tide gauge at Santa Monica (California, USA), but D.Cox arrived at the conclusion that it was a usual seishe and not the Indonesian tsunami.

1968, August 15, 6:14 a.m. (August 14, 22:14 p.m. GMT). There was a strong earthquake off the northwestern coast of Sulawesi Island. In the region of Manimbaha Bay (Tambu Bay in the map - authors' comment) between Tandjung, Manimbaha (the Manimbaya Cape limits the Tambu Bay from the south) and Sabang, displacements along faults caused the coast to subside by 2 - 3 m. A destructive tsunami arose. According to the Indonesian Hydrographic Service, waves 9 - 10 m high fell on the coast in the region of Donggala; they penetrated 500 m inland. 160 people died, 40 people where lost and 58 were injured; 800 coastal homes were destroyed and large areas of coconut plantations were flooded. The villages of Tambu and Mapaga (7 km north of Tambu) suffered especially). As a result of land subsidence Mapaga went underwater and even now, thirty years later, this picture is impressive.

Therefore, even a simple analysis of the available information on tsunami manifestations indicates a high level of tsunami hazard in the central part of Sulawesi Island. All the tsunamis occurred practically simultaneously with earthquakes, which leads to objective difficulties in developing a regional Tsunami Warning System and in employing the available the International Tsunami Warning System.

3. Earthquake of 01.01.96 and its manifestations

To estimate a tsunami focus one should have data on the earthquake mechanism and the geometry of its source. As is known, Indonesia is located at the intersection of three lithosphere plates: the Pacific plate, the Asian continental plate and the Indian-Australian plate. As a result, the frequency of earthquakes here is rather high. The Indonesian Meteorological and Geophysical Agency estimated the magnitude of the January 1, 1996 earthquake to be $M = 7$ on the open Richter scale, the epicenter coordinates being 0.60^0N, 119.92^0E, and the focus depth 39 km. The calculated earthquake epicenter was close to the zone of maximum destructions caused by the earthquake and tsunami in the Tonggolobibi village (the distance to the epicenter was 14 km). According to the data of the Harvard University provided at 24 stations, the earthquake had magnitudes $M_s = 7.7$ and $M_w = 7.8$ for surface waves and the magnitude $M_b = 6.4$ for body waves, the coordinates were $O.83^0$N, 120.01^0E, and the depth was 15 km. The seismic moment is estimated to be $5.5 \cdot 10^{27}$ dynes-cm. According to the Harvard University solution one of two possible fault planes could realise in the source: plate 1, strike 44°, dip 8°, slip 69°, and plate 2, strike 244°, dip 83°, slip 93°. In Dr. Gusyakov's

[3] The coordinates of this earthquake given in the catalog (see Table 2) are land ones (15 km east of Palu, approximately the same distance from the Tomini Bay).

opinion, the second variant was realised in this case, i.e. we dealt with a backarc thrust practically without a shear component along a steep (83°) fault N64E azimuth oriented plane.

On January 1 at 9:14 GMT (an hour after the mainshock) a rather strong aftershock with a magnitude 5.7 on the Richter scale occurred in the sea at 0.551°N, 119.897°E by the Harvard University estimates (by estimates of the Indonesian meteorological and geological agency the earthquake took place on land at 0.7°N, 120.3°E). In accordance with estimates of the Harvard University for the fault plane and the first aftershock coordinate, during the first hour the fault occurred in the direction of the Tonggolobibi village, which provided maximum shaking in this region.

All aftershocks (their coordinates are shown in Figure 4) in the central part of Sulawesi Island occurred within January, 1996 are given in Table 2 and characterise the seismic activity of the region (data of the United States Geological Survey, National Information Earthquake Center are provided by Dr. Gonzales).

Table 2

Data on aftershocks within January 1996

Date	Time (GMT)	Coordinates	Magnitude
January 1	08:05	0.83°N; 120.01°E	7.8
January 1	09:10	0.55°N; 119.9°E	5.7
January 7	01:34	0.3°N; 120.5°E	4.8
January 11	19:45	0.49°N; 119.5°E	5.3
January 13	04:27	0.3°N; 119.4°E	4.8
January 13	17:52	0.77°N; 120.2°E	4.7
January 27	19:14	0.98°N; 120.2°E	5.2
January 31	17:46	0.53°N; 119.65°E	4.7

The position and orientation of a tsunami focus is usually identified with the source of a tsunamigenic earthquake. Its equivalent radius R (in km) can be estimated by means of the regression dependence (Iida, 1963)

$$\log R = 0.5M - 2..2. \qquad (1)$$

and for M = 7.7 we obtain R = 45 km. An effective displacement of the water surface (or the sea bottom) H_e in the tsunami source can also be estimated using the empirical formula (Iida, 1962; Pelinovsky, 1982)

$$\log H_e = 0.8M - 5.6 \qquad (2)$$

where H_e is in meters. The sea bottom displacement in the source for M = 7.7 amounts to H_e = 3.6 m. Therefore, the sea bottom can move by 3.5 m in a tsunami source of a radius approximately equal to 45 km. For these sizes the earthquake and tsunami source extends to the land, which is confirmed by destructions of houses in the Tonggolobibi village and in other places (the earthquake intensity is maximum in the coastal zone and is rated 6 on the Modified Mercalli scale). Besides in the region to the west of the Tonggolobibi village, native people observed land subsidence by almost 1 m, which also corresponds to the above estimates. In particular, a coral reef edge on Pangalaseang could serve as a rule of sea level; by eyewitness accounts it subsided by approximately 70 cm (judging by tide observations).

4. Measurement of tsunami wave runup

Instrumental measurements of maximum heights of tsunami runups were carried out at 16 points on a shore about 100 km long between Pangalaseang Island and the Simuntu village. Coordinates of each measurement point were determined by using a global position system (GPS). Practically everywhere the runup heights were measured by means of clearly visible tsunami marks on walls of houses (Figure 4) or a clearly visible boundary of scattered things: grass, trees, pieces of walls (Figure 5). All heights of runups were corrected for the precalculated tide height at the measurement instant which, naturally, did not take into account a possible subsidence caused by an earthquake (tide tables of the Navy Hydro-Oceanographic Service were used). The measurement results are summarised in Table 3 and shown in Figure 6. As is seen, the maximum tsunami height at different points varied within 1.62 - 3.43 m above sea level. The highest tsunami was in the Tonggolobibi village and to the west of it, i.e. in the region identified with the tsunami source. The density of

the distribution function of the runup heights along the coast is practically constant and the integral distribution function in the range 1.62 - 3.43 m is approximated by the linear law (Figure 7)

$$P = 1.73 - 0.47H\,. \qquad (3)$$

Table 3

Maximum runup heights of tsunami waves (above mean sea level)

North Latitude	East Longitude	Point	Height (m)
00°28'57.8''	119°54'25.1''	Pangalaseang Island	2.28
00°28'34.2''	119°55'50.9''	Munte	3.17
00°28'26.4''	119°56'51.9''	Limbosu	2.81
00°28'33.5''	119°57'27.8''	Tonggolobibi	1.82
00°28'45.2''	119°58'35.6''	Tonggolobibi	3.37
00°28'51.4''	119°58'41.3''	Tonggolobibi	3.43
00°28'58.8''	119°59'30.0''	Taipah (river mouth)	2.48
00°28'58.4''	119°59'51.4''	Taipah	3.19
00°28'58.8''	119°59'52.0''	Taipah	3.25
00°29'03.4''	120°00'11.9''	Taipah	2.40
00°29'59.6''	120°01'38.8''	Siboang	1.78
00°33'03.6''	120°02'19.9''	Siwalempu	1.62
00°34'52.8''	120°02'13.0''	Balukang	2.52
00°45'57.2''	120°11'27.7''	Soni	1.79
00°49'15.3''	120°14'41.6''	Dongko	2.39
00°53'42.2''	120°14'14.6''	Simuntu	2.00

An average runup height along the whole part of the shore is H = 2.5 m with a standard deviation of 0.6 m. The latter permits to evaluate the tsunami magnitude using the formula (Soloviev, 1972)

$$I = 0.5 + \log_2 H\,, \qquad (4)$$

yielding I = 1.8. It should be noted that when analysing historical data Soloviev indicates the maximum intensity value of I = 2 for Sulawesi and Kalimantan Islands and our value for the 01.01.96 event proves to be close to it. Unfortunately, we yet do not have tide-gauge records at our disposal (in particular, on the Palu Bay and Kalimantan Island) which could supplement the tsunami characteristics measured on land.

It is noteworthy that the tsunami came at the instant of a high water (at the instant of the earthquake its precalculated value amounted to 59 cm above mean sea level). The tidal component at the earthquake instant is often neglected in literature and the runup height of the tsunami wave is given "in the pure form". Taking into account this correction the maximum tsunami height varies from 1.03 m to 2.84 m (the average value is 1.93 that is approximately twice as large as the estimated value of the tsunami height in the source). However, it should be kept in mind that the interaction between a tsunami wave and a tide is, in general, of the nonlinear character, especially in the region near the water edge, thus the accuracy of various correcting values of runup heights cannot be very high.

In the region of the Taiphan village we found three clearly visible lines on a house wall, they are tsunami marks spaced at 1 and 15 cm. This means that the tsunami was at least three waves, which is confirmed by eyewitness accounts.

Table 4

Measured wave heights and visual estimates

Point	Visual estimate of height (m)	Measured height (m)
Tonggolobibi	2	2.87 (average)
Siboang	1.5	1.78
Siwalempu	1.5	1.62
Babukang	1.25	2.52

It is important for practical purposes to compare measured heights of tsunami wave runups with data given in various regional documents and sources (visual estimates, tide is not taken into account). The results of the comparison are presented in Table 4. As is seen, the measurements yield larger values of wave heights than the visual estimates. The proportionality factor equals approximately 1.4 with deviation ± 0.4. It is of extreme importance to make such a comparison for other tsunamis in order to determine the degree of confidence in visual measurements of tsunami wave heights.

5. Reports of eyewitnesses

Accounts of eyewitnesses provide additional data on characteristics of tsunami waves, in particular, on arrival time of waves, their quantity, number of maximum amplitude wave, wave period, character of wave runup, sea recession before wave arrival, etc. The available data are accumulated in Table 5. Therefore, on the average, three tsunami waves with a period 1 - 3 min climbed up the populated localities, the first and second waves being maximum. The wave arrived in 5 - 10 min after the earthquake. It was observed that in three cases a tsunami was preceded by the sea recession from the shore. The wave usually broke down on a spit shielding the villages from the sea side. The wave stand for about 15 min (in low-lying places). Note also that it rained heavily during the tsunami.

Table 5

Tsunami wave characteristics provided by eyewitness accounts

Locality	Quantity of waves	Number of maximum amplitude wave	Arrival time (min)	Wave period (min)	Sea recession	Wave breaking
Pangalaseang Is.			10			–
Munte	3	2			+	–
Limbosu	3	1				
Tonggolobibi	3		5-7			
Taipah	3	2	5-7	1	+	–
Siboang	7	1			–	
Siwalempu	3	3	5		+	+
Balukang	4	1 or 2	5	2-3		+
Soni	3	1	1-5	1		+
Dongko	3	2	10			
Simuntu	3	2				

Let us make some estimates based on the available data. The water depth at the earthquake epicenter exceeds 200 m (the epicenter is on a slope between the isobaths of 200 and 1400 m). Assuming that the period and the wavelength (the size of the source) are related by the formula of the linear theory for long waves

$$T = R / \sqrt{gh} \qquad (5)$$

(where g is the acceleration of gravity), and taking an average depth in the source to be equal to 800 m, we estimate from (5) the tsunami wave period T = 4 min that is close to the observed value. The time of the tsunami wave arrival is larger than the wave period due to slower wave propagation in shallow water and has the order of 5 - 10 min that is also close to the values given by tsunami eyewitnesses.
The character of the tsunami wave runup depends on the breakdown parameter (Pelinovsky, 1982)

$$Br = \frac{\omega^2 H}{g\alpha^2}, \qquad (6)$$

where α is the shore slope and ω is the wave frequency. If $Br > 1$, the wave breaks down. Assuming that H = 3 m, the wave period is 100 s and the bottom slope is 1/20, we obtain from (6) Br = 0.5 that is close to the

transition value. Thus, the wave breakdown may occur at steep acclivities, which is confirmed by eyewitness accounts.

6. Tsunami action on shores and installations

As a rule, coastal villages are separated from the sea by natural sand dams whose height can achieve 1 - 2 m. The characteristic transverse profiles of the coastal zone are shown in Figure 8. Being struck by tsunami waves, the relief of the water edge region varies during a tsunami, in particular, tsunami eyewitnesses evidence that the height of natural dams decreased approximately by 1 m after a tsunami. Unfortunately, we are unable to separate the processes of the land subsidence as a result of an earthquake and the sand material erosion in natural dams. Only on Pangalaseang Island the vertical displacement of a coral reef edge by 70 cm described by eyewitnesses can be related in the pure form to the land subsidence. It can be assumed that sand dams higher than 70 cm change their height by 30 - 50 cm due to erosion of the sea shore caused by tsunami waves. It should be noted that on Sulawesi Island, as well as in most part of Indonesia, wind waves are practically absent (they are the main factor of the sea shore erosion in other regions), that is why Indonesia is a unique ground for investigating sediment transport by tsunami waves. Part of the coast covered with fresh wet sand in the region of the Pangalaseang village is shown in Figure 9. An analogous photograph of Java Island demonstrating the action of the tsunami of June 2, 1994 is also given (Figure 10). Much attention is paid now to these processes in relation to the study of paleotsunami traces (Minoura and Nakaya, 1991), mathematical models of the phenomenon are also being developed (Pelinovsky, Talipova, 1994). One more example of sediment transport in tsunami waves is the sand scouring near a building foundation resulted in destruction of a concrete wall of the building in the Taipah village during the tsunami wave ebb (according to witness accounts).

The destructive force of a tsunami, naturally, depends on the relief of land, in particular, in river beds a tsunami travelled large distances (of the order of 200 m), it carried several boats to the shore. Such phenomena were present practically in all tsunamis. A tsunami manifested itself most strongly together with an earthquake on land in the Tongolobibi village: it broke all houses in one part and killed some people, this part is shown in Figure 11. In other places, judging by marks on walls of houses, a height of a water flow on the shore was of the order of H = 1 m (Figure 4). The velocity of its movement can be found by the formula (Murty, 1977)

$$c = (1 \div 2)\sqrt{gH} \qquad (7)$$

and it does not exceed 5 m/s. This velocity enabled many eyewitnesses of tsunami to escape from it.

And finally, the relatively small height of the water flow in many populated localities stimulates a more thorough consideration of the role of tides for estimating the shore zone flooded by tsunami waves. The tsunami wave came at the instant of high water (59 cm above average sea level) and it caused strong destructions. For low water the sea level lowers by 1.3 m, i.e. the water level difference amounts to 1.89 m. This means that if an earthquake had occurred at the time of an ebb, the tsunami would practically have been invisible in all populated localities, except for river beds and the part of the Tongolobibi village.

7. Estimation of tsunami risk in central part of Sulawesi Island

The information on tsunami parameters obtained within the survey and the historical data given in Table 1 enable us to make a rough estimate of tsunami risk in the central part of Sulawesi Island. This estimate is based on the tsunami height exceedance frequency: the number of observed cases of tsunami with maximum height larger than that assigned for the observation period. In our case we have four tsunamis during 100 years and the corresponding values of the exceedance frequency are shown in Figure 12. These data are well approximated by the Poisson curve

$$f = 0.05\exp(-0.1H), \qquad (8)$$

where H is in meters and f is in 1/year. Simple estimates obvious from Table 1 show that a tsunami about 2 m high can be expected each 25 years, while a tsunami 15 m high once each 100 years.

8. Conclusions

The 01.01.1996 earthquake was one of the largest earthquakes in recent years in central part of Sulawesi Island. The survey team employed the same methods and requirements as in the other international surveys. The main conclusions of this survey are as follows:

1. The necessity of antiseismic high-quality construction should be stressed once again. Survey of attacked zones shows that dilapidated houses were most severely damaged. Many houses on Sulawesi Island are built on piles which, on the one hand, helps at small tsunami heights (the survey has revealed many such cases) and, on the other hand, their quality is insufficient and houses are destroyed by earthquakes or earth washing-out by tsunamis. Taking into account that tsunamis occur relatively rarely (once each 25 years), village construction planning does not foresee inundation and many houses are in a potentially dangerous zone. Some experience of such construction planning has been gained in Russia where a preliminary map of Far East tsunami zoning has been created and this experience can be used in Indonesia.
2. An earthquake 01.01.96 occurred in the immediate vicinity from the coast, so that tsunamis arrived practically at the same time. This circumstance gives no way of warning population about the tsunami. It should be note that all tsunamis on Sulawesi Island (in its central part) occurred simultaneously with earthquakes and could not be prevented using standard methods (after the earthquake onset). The only way out is teaching residents to survive in such extreme situations and this is recommended by the International Tsunami Commission. But, in fact, teaching is not effective in Indonesia as in Russia.
3. The survey conditions on Sulawesi Island were close to traditional survey conditions on the Kuril Islands in Russia . In particular, during the winter season of rains many roads became impassible and were blocked with landslides, thus there were some transportation problems: waiting for a plane during several days, impossibility to visit some places because of landslide danger. Cars, motor cycles and boats were used in the survey. Assistance provided by official authorities and army often proved to be a decisive factor for successful investigation and this was demonstrated by this survey.
4. High frequency of tsynamigenic earthquakes on Sulawesi Island (not only in its central part) enabled Prof. Soloviev (1972) to single out Sulawesi in a separate zone when comparing data on earthquakes and tsunamis in various parts of the Pacific. From the viewpoint of long-term tsunami prediction, Sulawesi Island has the same values of predicted wave heights as the Kuril Islands in Russia. Thus, the wave heights on Sumshu and Paramushir Islands predicted for 100 years are 9 and 17 m (Go et al., 1988), while on Sulawesi Island 15 m.
5. An important problem encountered by different survey teams is taking into account of land subsidence during a tsunamigenic earthquake. This characteristic was measured by a special survey during the Shikotan tsunami 04.10.1994 (the island subsided by 53 cm). Visual low-accurate estimates of such subsidence are usually used in tsunami investigation practice. As a result, high accuracy of wave height measurements with account of tides is "impaired" by low accuracy of land subsidence measurements. This issue requires special consideration, since appropriate measurement need different equipment and larger financial investments. However, its solution is principal for numerical tsunami simulation and choice of more adequate models.

Acknowledgements

The survey was partially supported by the Russian Foundation of Basic Research (grant No. 96-5-167286) and the Indonesian Tsunami Research Center. Valuable information on earthquake characteristics on Sulawesi Island provided by Dr. F.Gonzalez (USA) is highly appreciated by the authors. Advices of Drs. B.Levin and V.Gusyakov are of special value. The authors wish to thank A.Stromkov, M.Zubov and V.Pelinovskaya for assistance in preparing illustrations and N.Rudik for translation of manuscript. Theoretical part of the study was supported by RFBR grant (No. 96-05-64111). Measurement data are included in information tsunami system being developed under the support of RFBR grant (No. 95-07-19335).

References

Choi, B., Pelinovsky, E. et al.: 1994, Tsunami Survey of East Coast of Korea due to the 1993 Southwest of the Hokkaido Earthquake. *J. Korean Soc. Coastal and Ocean Engn.*, **6**, 117 - 125.

Foley, G.: 1994, The Tsunami Event along the Northwest Australian Coast on 3 June 1994. *National Tsunami Workshop*, Brisbane, 25 - 31.

Go, Ch.N., Kaistrenko, V.M., Pelinovsky, E.N., and Simonov, K.V.: 1988, A quantitative estimation of tsunami hazard and tsunami zonning scheme of the Pacific coast of the USSR. *Pacific Annual*, Vladivostok, 7 - 15.

Iida, K.: 1963, A relation of earthquake energy to tsunami energy and the estimation of the vertical displacement in a tsunami source. *J. Earth Sci. Nagoya Univ.*, **11**, 49 - 67.

Minoura, K., and Nakaya, S.: 1991, Tracers of Tsunami Preserved in Inter-tidal Lacustrine and Marsh Deposits: Some examples from Northeast Japan. *J. Geology*, **99**, 265 - 287.

Murty, T.S.: 1977, *Seismic Sea Waves - Tsunami*. Bull. Fish. Res. Board Canada, No. 198.

Pelinovsky, E.N.: 1982, *Nonlinear Dynamics of Tsunami Waves*. Gorky, Applied Physics Institute Press. (in Russian)

Pelinovsky, E., and Talipova, T.: 1994, Sediment Transport Model for Tsunami Waves. Abstracts of the 1994 AGU Fall Meeting. *EOS.*, **75**, N. 44, Suppl. 356.

Prasetya, G.S., and Jumadi, R.H.: 1995, Report on Survey of Coastal land subsidence caused by East Timor Earthquake May 14, 1995. BPPT, Jakarta. (unpublished).

Soloviev, S.L.: 1972, Reccurence of earthquakes and tsunamis in the Pacific Ocean. In *Tsunami Waves* (Proc. SakhKNII), Sakhalin, 7 - 47. (in Russian)

Soloviev, S.L., and Go, Ch.N.: 1984, *Catalogue of tsunamis on the western shore of the Pacific Ocean.* Canada institute for Scie. and tech. Information, Ottawa.

Soloviev, S.L., Go, Ch.N., and Kim, Kh.S.: 1992, *Catalog of tsunamis in the Pacific 1969 - 1982.* Soviet Geophysical Committee, Moscow.

Yeh, H., Imamura, F., Synolakis, C., Tsuji, Y., Liu, P., and Shi, S.: 1993, The Flores Island Tsunamis. *EOS, Transactions*, , **74**, 369, 371 - 373.

Yeh, H., Titov, V., Gusiakov, V., Pelinovsky, E., Khramushin, V., and Kaistrenko, V.: 1995, The 1994 Shikotan Earthquake Tsunamis. *PAGEOPH*, **144**, 855 - 874.

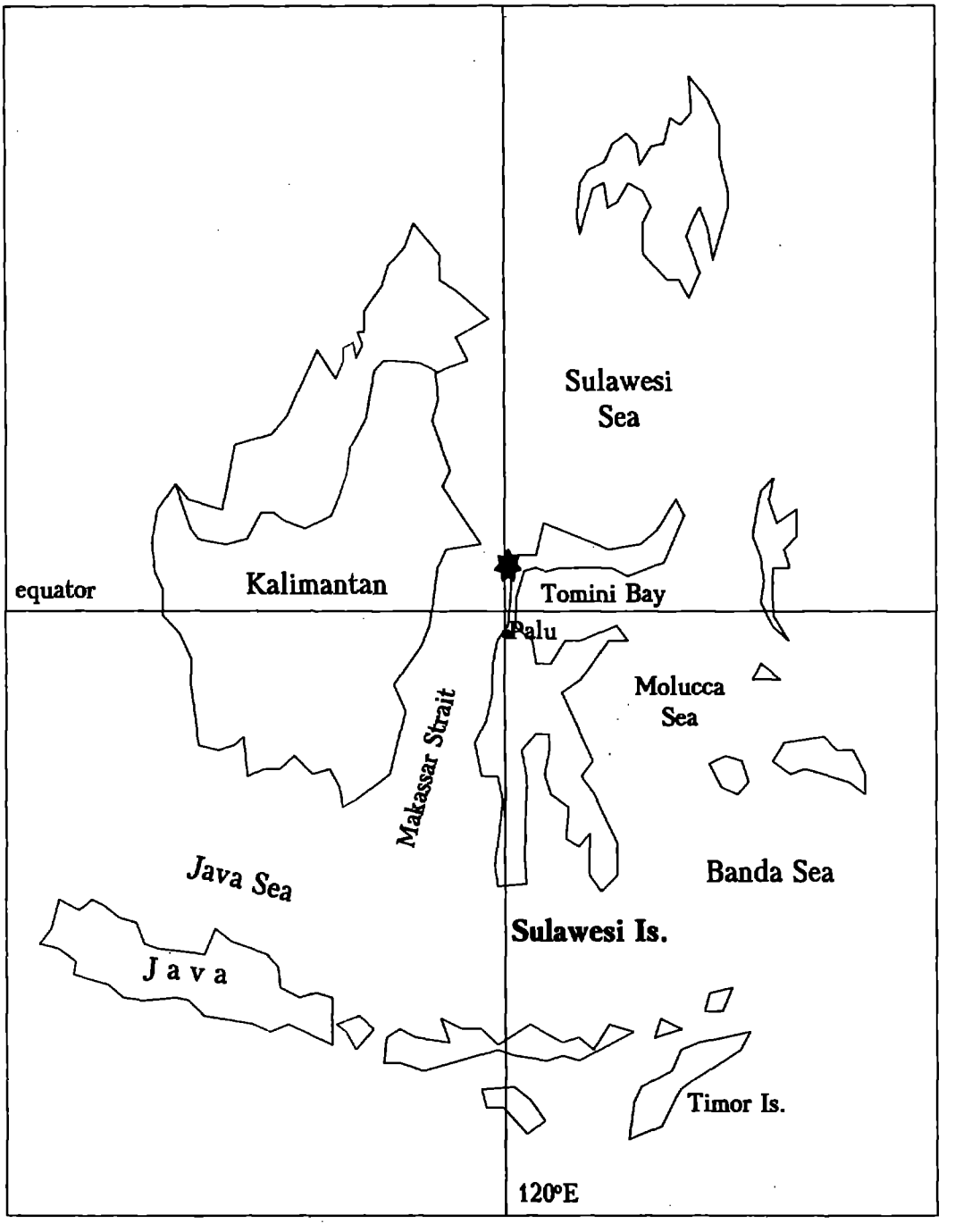

Fig. 1. Map of Indonesia with marked position of January 1, 1996 earthquake.

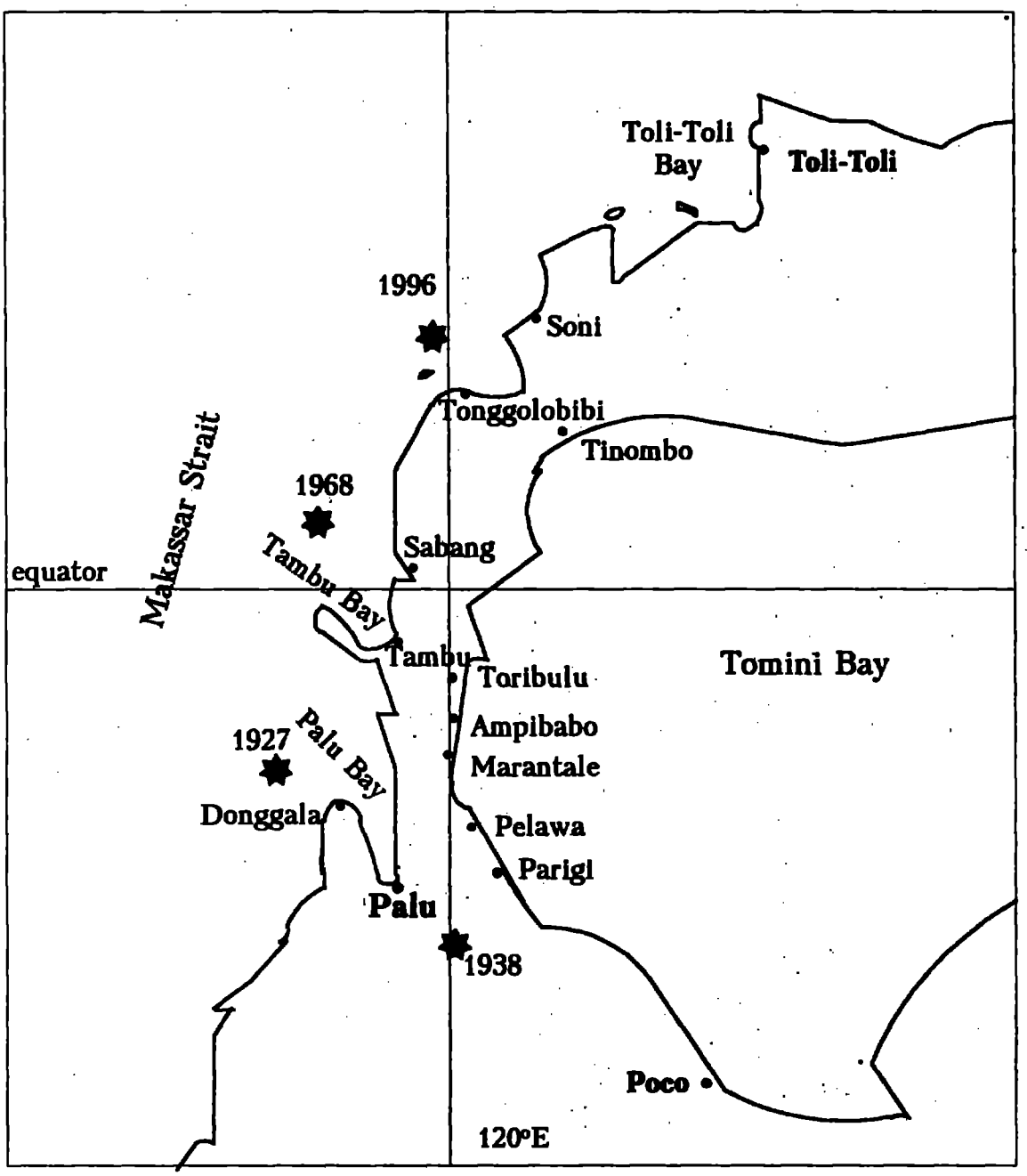

Fig. 2. Epicenters of tsunamigenic earthquakes of this century in the central part of Sulawesi.

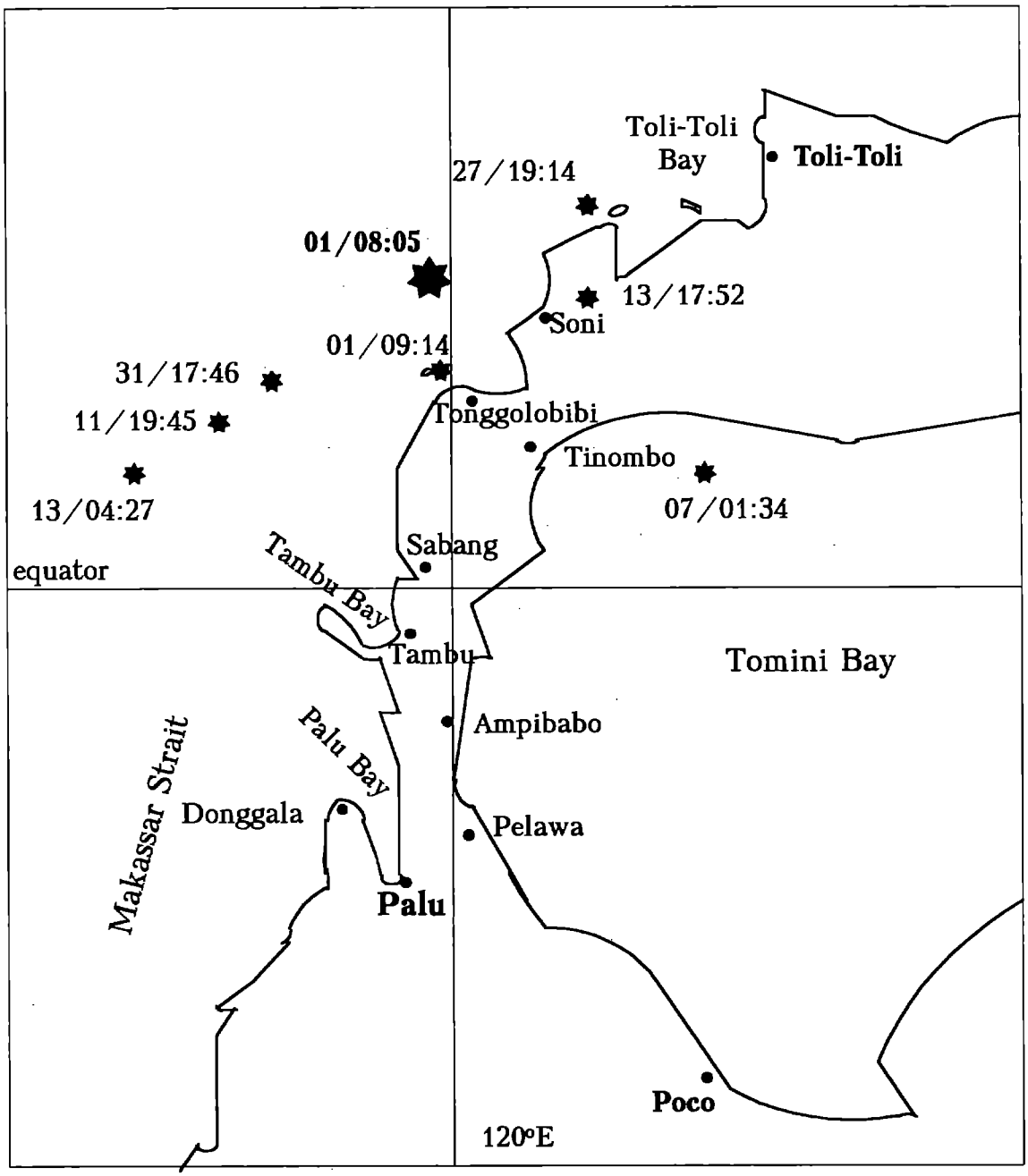

Fig. 3. Epicenter and aftershocks of January 1, 1996 earthquake.

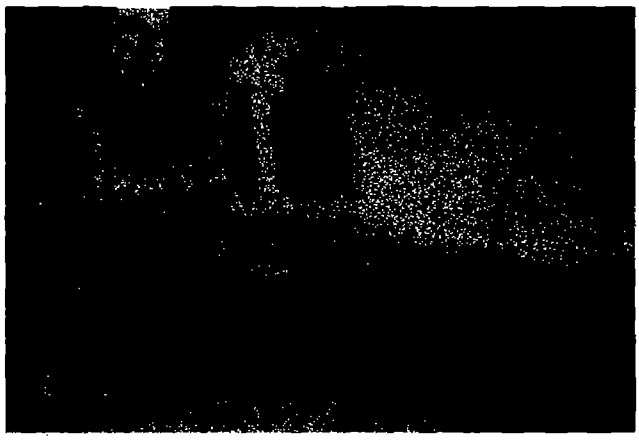

Fig. 4. Tsunami mark on a house wall.

Fig. 5. Scattered trees at the flooded zone boundary.

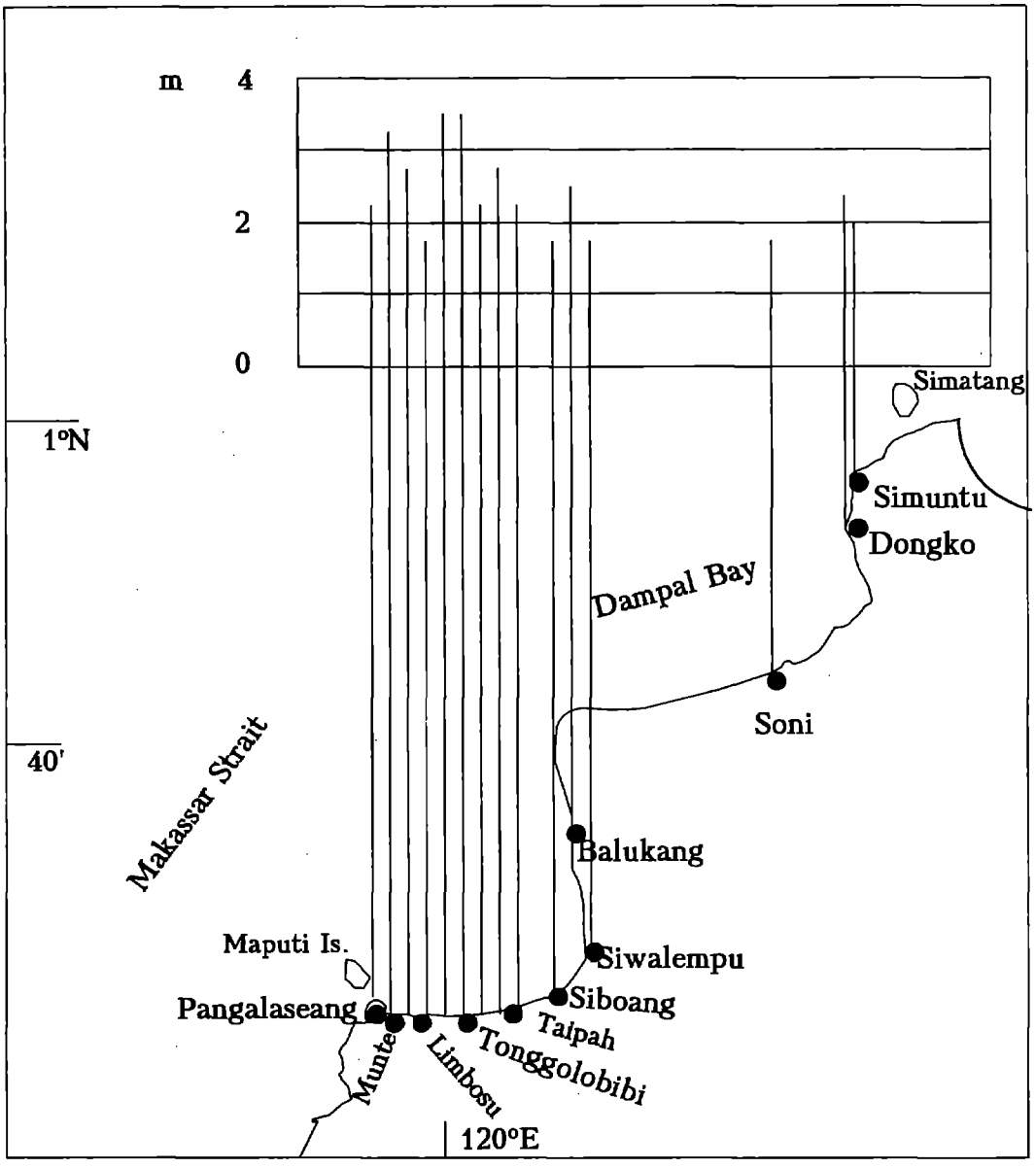

Fig. 6. Distribution of runup heights along the coast.

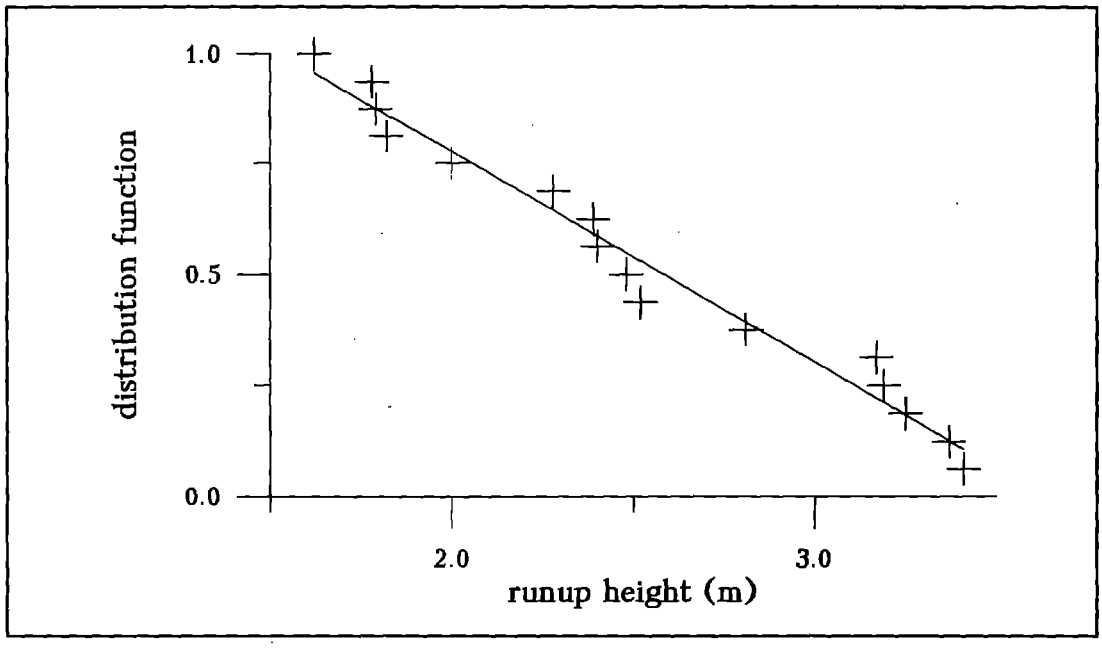

Fig. 7. Distribution function of runup heights.

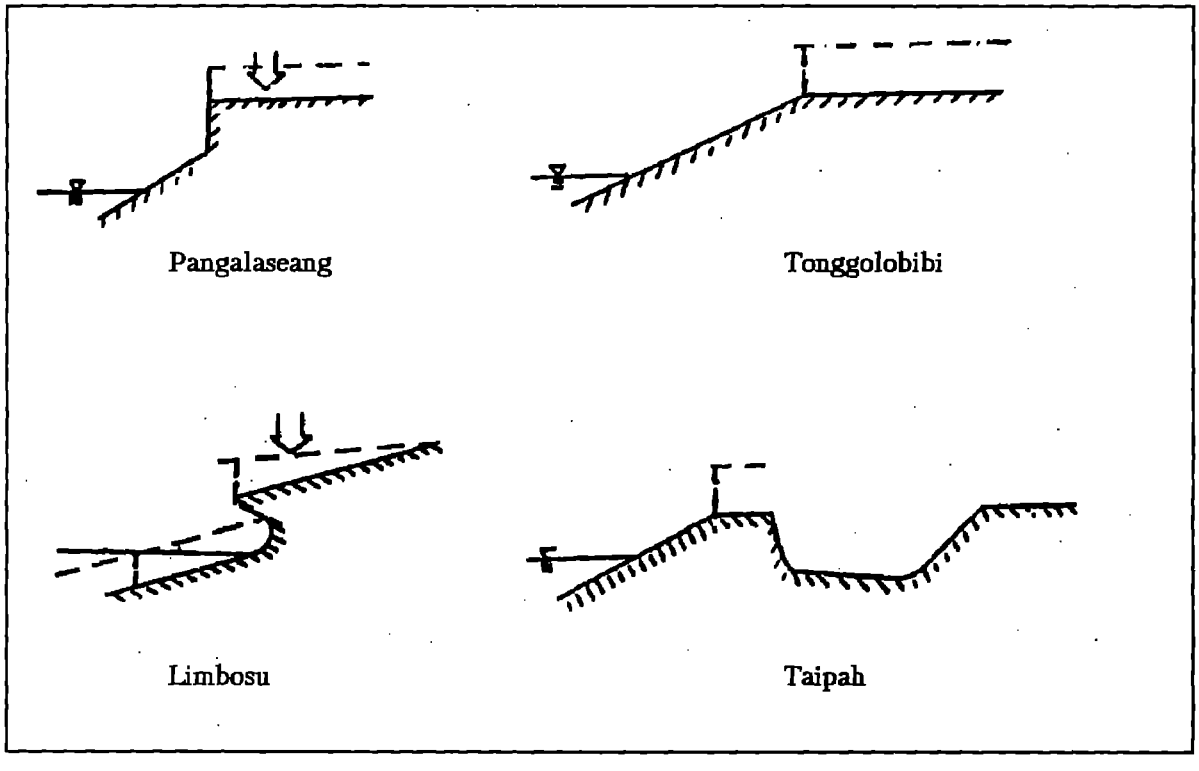

Fig. 8. Transverse profiles of the coast.

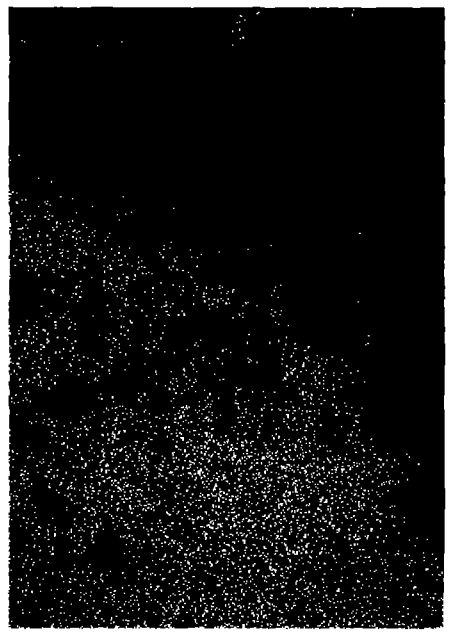

Fig. 9. Sand transported from sea by tsunami waves

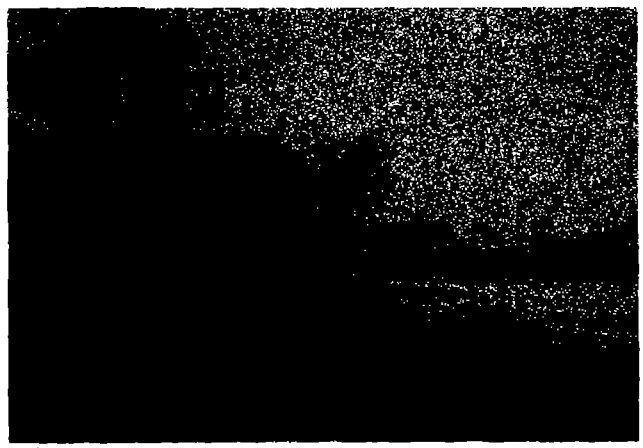

Fig. 10. Sand transported from sea by a wave during the 02.06.94 Java tsunami.

Fig. 11. Zone of maximum destructions in the Tonggolobibi village.

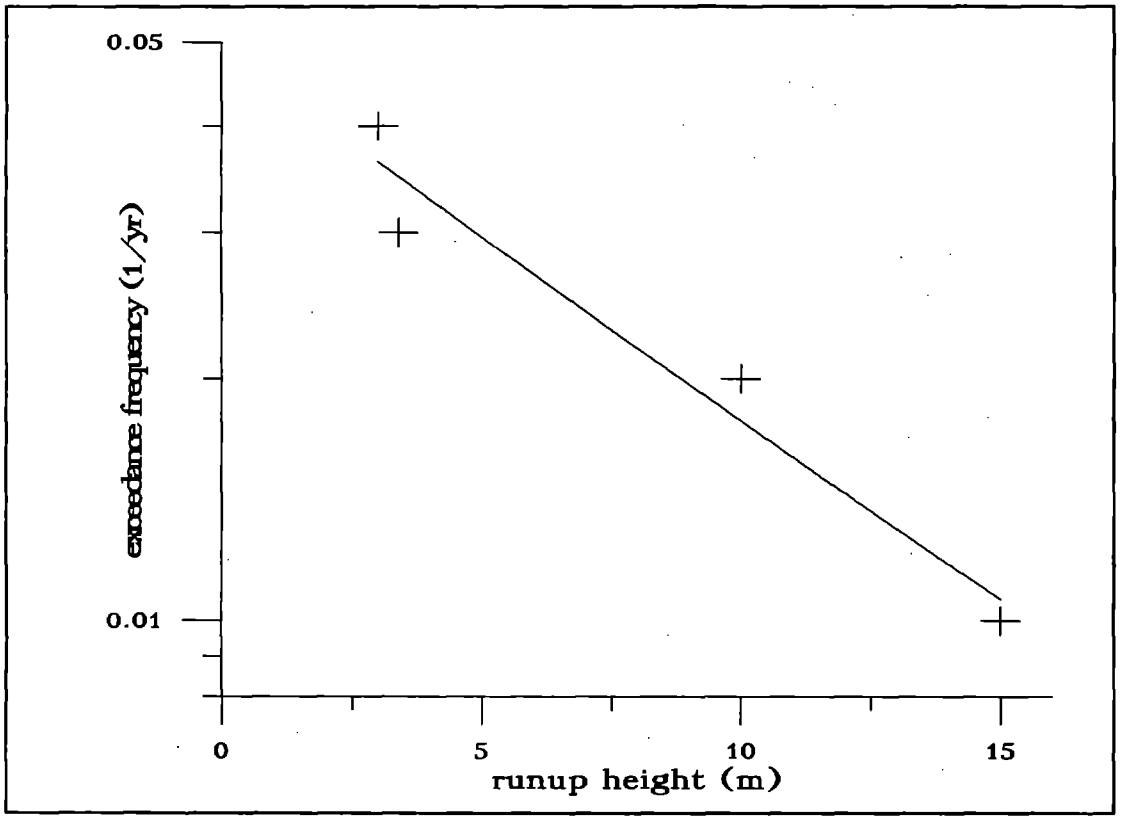

Fig. 12. Exceedance frequency of tsunamis in central part of Sulawesi Island.

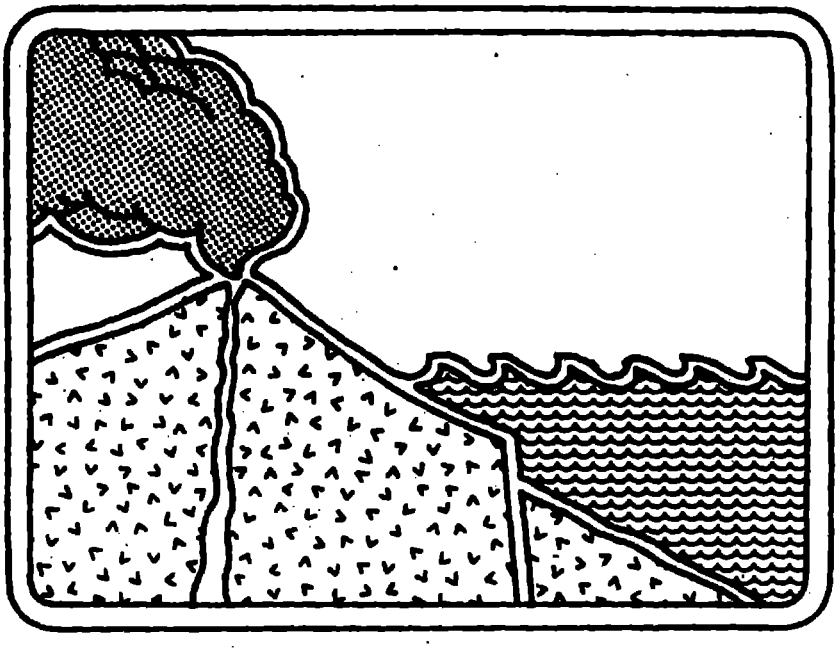

TSUNAMI WEB SITE DIRECTORY

A web site with the listing of all the papers published during the last 15 years of *Science of Tsunami Hazards* is being published by Dr. Antonio Baptista. The web site has the following URL:

http://www.ccalmr.ogi.edu/STH

Any author who wishes to have his entire paper on the web site should make arrangements with the web site publisher, Dr. Antonio Baptista at :baptista@ccalmr.ori.edu.

The International Tsunami Information Center maintains a web site with current information of interest to the Tsunami community. The new director of ITIC, Mr. Michael Blackford plans to expand the tsunami news section on the web site. The web site has the following URL:

http://tgsv5.nws.noaa.gov/pr/hq/itic.htm

The West Coast and Alaska Tsunami Warning Center maintains a web site with tsunami information. The web site has the following URL:

http://www.alaska.net/~atwc/

A web site about Tsunamis is being published by **Tsunami Society** member, Dr. George Pararas-Carayannis. His tsunami web site has the following URL:

http://www.geocities.com/capecanaveral/lab/1029

A web site about The National Tsunami Hazard Mitigation Program is maintained by **PMEL**. The web site has the following URL:

http://www.pmel.noaa.gov/tsunami-hazard

Several members of **The Tsunami Society** have helped develop a web site for the **Pacific Tsunami Museum** in Hilo, Hawaii. The web site has the following URL:

http://planet-hawaii.com/tsunami

Any other **Tsunami Society** member who is publishing tsunami information on a web site may wish to inform the Editor so that it may be included in future tsunami web site directories.

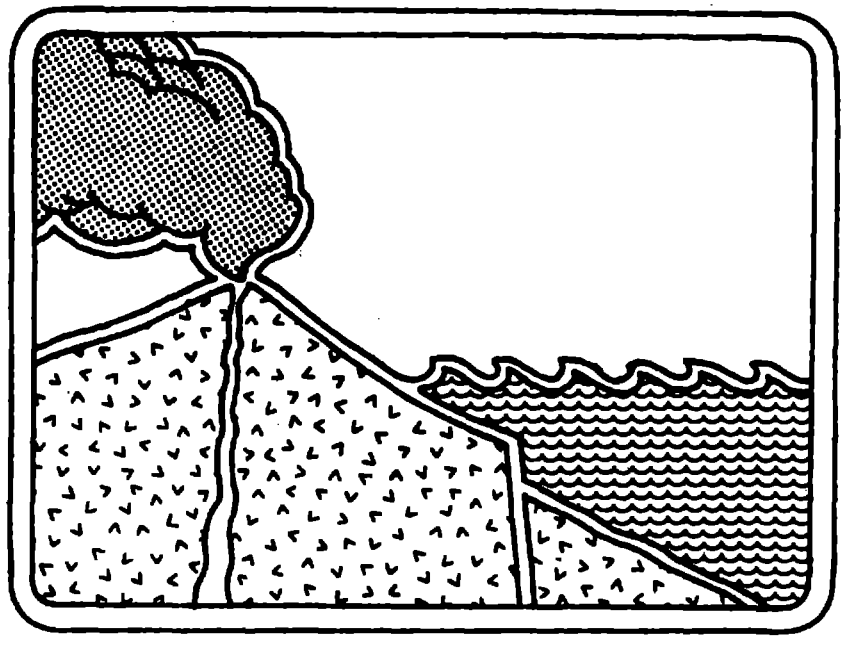

OBJECTIVE: **The Tsunami Society** publishes this journal to increase and disseminate knowledge about tsunamis and their hazards.

DISCLAIMER: Although these articles have been technically reviewed by peers, **The Tsunami Society** is not responsible for the veracity of any statement, opinion or consequences.

Submit manuscripts of articles, notes or letters to the Editor. If an article is accepted for publication the author(s) must submit a camera ready manuscript in the journal format. A voluntary $50.00 page charge will include 50 reprints.

SUBSCRIPTION INFORMATION: Price per copy $20.00 USA

ISSN 0736-5306 **http://www.ccalmr.ogi.edu/STH**

Published by The Tsunami Society in Honolulu, Hawaii, USA